

SERENADE: A Parallel Randomized Algorithm Suite for Crossbar Scheduling in Input-Queued Switches

Long Gong[†] Liang Liu[†] Sen Yang[†]
gonglong@gatech.edu lliu315@gatech.edu sen.yang@gatech.edu

Jun (Jim) Xu[†] Yi Xie[‡] Xinbing Wang^{††}
jx@cc.gatech.edu csyxie@xmu.edu.cn xwang8@sjtu.edu.cn

May 12, 2022

Abstract

Most of today’s high-speed switches and routers adopt an input-queued crossbar switch architecture. Such a switch needs to compute a matching (crossbar schedule) between the input ports and output ports during each switching cycle (time slot). A key research challenge in designing large (in number of input/output ports N) input-queued crossbar switches is to develop crossbar scheduling algorithms that can compute “high quality” matchings – *i.e.*, those that result in high switch throughput (ideally 100%) and low queueing delays for packets – at line rates. SERENA is arguably the best algorithm in that regard: It outputs excellent matching decisions that result in 100% switch throughput and near-optimal queueing delays. However, since SERENA is a centralized algorithm with $O(N)$ computational complexity, it cannot support switches that both are large (in terms of N) and have a very high line rate per port. In this work, we propose SERENADE (SERENA, the Distributed Edition), a parallel algorithm suite that emulates SERENA in only $O(\log N)$ iterations between input ports and output ports, and hence has a time complexity of only $O(\log N)$ per port. Through extensive simulations, we show that all three variants in the SERENADE suite can, either provably or empirically, achieve 100% throughput, and that they have similar delay performances as SERENA under heavy traffic loads.

1 Introduction

The volumes of network traffic across the Internet and in data-centers continue to grow relentlessly, thanks to existing and emerging data-intensive applications, such as Big Data analytics,

[†]Georgia Institute of Technology, USA

[‡]Xiamen University, China

^{††}Shanghai Jiao Tong University, China

cloud computing, and video streaming. At the same time, the number of network-connected devices also grows explosively, fueled by the wide adoption of smart phones and the emergence of the Internet of things. To transport and “direct” this massive amount of traffic to their respective destinations, routers and switches capable of connecting a large number of ports and operating at very high per-port speeds are badly needed.

Most of today’s switches and routers adopt an input-queued crossbar switch architecture. Figure 1 shows a generic input-queued switch employing a crossbar to interconnect N input ports with N output ports. Each input port has N Virtual Output Queues (VOQs). A VOQ j at input port i serves as a buffer for the packets going into input port i destined for output port j . The use of VOQs solves the Head-of-Line (HOL) blocking issue [21], which severely limits the throughput of the switching system.

1.1 Matching Problem and SERENA Algorithm

In an input-queued crossbar switch, each input port can be connected to only one output port, and vice versa, in each switching cycle, or time slot. Hence, it needs to compute, per time slot, a one-to-one *matching* between input and output ports. The primary research challenge in designing large (in number of input/output ports N) input-queued crossbar switches is to develop algorithms that can compute “high quality” matchings – *i.e.*, those that result in high switch throughput (ideally 100%) and low queueing delays for packets – at line rates.

Unfortunately, there appears to be a tradeoff between the quality of a matching and the amount of time needed to compute it (*i.e.*, time complexity). Maximum Weight Matching (MWM), with a suitable weight measure such as VOQ length, is known to produce empirically optimal matchings in terms of queueing delay, for a large variety of traffic patterns [28, 34]. Each matching decision however takes $O(N^3)$ time to compute [11].

Researchers have been searching for crossbar scheduling algorithms that have time complexity much lower than $O(N^3)$, but performance close to MWM. So far, the best such approximation to MWM is SERENA [14, 33]. SERENA produces excellent matching decisions that result in 100% switch throughput and queueing delay close to that of MWM. However, it is a centralized algorithm with $O(N)$ time complexity. When N is large, this complexity is too high to support very high link rates. Hence, as stated in [14, 33], SERENA is designed for high-aggregate-rate switches – *i.e.*, those that have either a large number of ports or a very high line rate per port – but not for those that have both. While parallelizing the SERENA algorithm seems to be an obvious solution to this scalability problem, we will show in §3.2 that

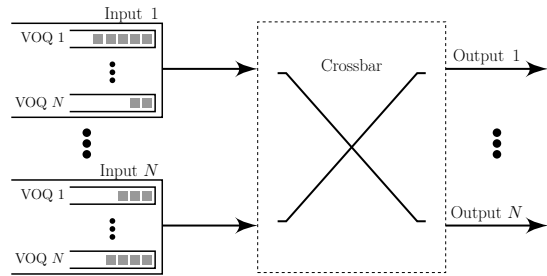


Figure 1: An input-queued crossbar switch.

a key procedure in SERENA, namely MERGE, is monolithic in nature, making SERENA hard to parallelize.

1.2 Parallelizing SERENA via SERENADE

In this work, we propose SERENADE (SERENA, the Distributed Edition), a parallel algorithm suite that emulates each matching computation of SERENA using only $O(\log N)$ iterations between input ports and output ports. Hence, each input or output port needs only to do $O(\log N)$ work to compute a matching, making SERENADE scalable in both the switch size and the line rate per port. The SERENADE suite contains three basic variants: E-SERENADE (E for Exact), C-SERENADE (C for Conservative), and O-SERENADE (O for Opportunistic). E-SERENADE exactly emulates SERENA in no more than $1.5 \log_2 N$ iterations on average. In comparison, C-SERENADE and O-SERENADE both only approximately emulate SERENA in $1 + \log_2 N$ iterations. However, the delay performance of O-SERENADE is very close to that of SERENA, under various traffic workloads, and that of C-SERENADE is under heavy traffic workloads. Here we drop the “big O ” notations in counting the number of iterations in all three SERENADE variants, emphasizing the constant factors.

SERENADE overcomes the aforementioned challenge of parallelizing SERENA, namely the monolithic nature of the MERGE procedure, by making do with less. More specifically, we will show in [Appendix B](#) that, in any SERENADE variant, after its $O(\log N)$ iterations, each input port has much less information to work with than the central processor in SERENA; yet all SERENADE variants can make matching decisions either exactly or almost as wise as SERENA. In other words, SERENADE does not precisely parallelize SERENA, in that it does not duplicate the full information gathering capability of SERENA; rather, it gathers just enough information needed to make a matching decision that is either exactly or almost as wise. This making do with less is a major innovation and contribution of this work.

SERENADE, by “converting” the sequential algorithm SERENA that has $O(N)$ time complexity to a parallel iterative algorithm that requires only $O(\log N)$ iterations, also has the following profound implication. By far the best known among parallel iterative crossbar scheduling algorithms is iSLIP [\[27\]](#), in which input and output ports compute a matching also through $O(\log N)$ iterations. However, iSLIP computes a different type of matching called Maximum Cardinality Matching (MCM), which is of lower quality than MWM. Hence iSLIP cannot achieve 100% throughput except under the uniform traffic pattern, and has much longer queueing delays than SERENA under heavy nonuniform traffic. SERENADE gets the better of both worlds: Its time and communication complexities are comparable to iSLIP’s, yet its throughput and delay performances are either identical or close to SERENA’s.

The rest of the paper is organized as follows. In [§2](#), we offer some background on input-queued crossbar switches. In [§3](#), we describe in detail the MERGE procedure in SERENA that is to be parallelized in SERENADE. In [§4](#), we describe the common initial stage of all three SERENADE variants, before zooming in on these variants in [§5](#). In [§6](#), we introduce two hybrid

SERENADE schemes that “mix” a tiny amount of E-SERENADE with C-SERENADE and O-SERENADE. In §7, we evaluate the performance of SERENADE. In §8, we provide a brief survey of related work before concluding the paper in §9.

2 System Model and Background

We assume that all incoming variable-size packets are segmented into fixed-size packets, which are then reassembled when leaving the switch. Hence we consider the switching of only fixed-size packets in the sequel, and each such fixed-size packet takes exactly one time slot to transmit. We also assume that both the output ports and the crossbar operate at the same line rate as the input ports. Both assumptions above are widely adopted in the literature [14, 17, 27–29].

An $N \times N$ input-queued crossbar switch is usually modeled as a weighted complete bipartite graph $G(I \cup O)$, with the N input ports and the N output ports represented as the two disjoint vertex sets $I = \{I_1, I_2, \dots, I_N\}$ and $O = \{O_1, O_2, \dots, O_N\}$ respectively. Each edge (I_i, O_j) corresponds to the j^{th} VOQ at input port i and its weight is defined as the number of packets in the VOQ.

A valid schedule, or *matching*, is a set of edges between I and O in which no two distinct edges share a vertex. The weight of a matching is defined as the total weight of all edges belonging to the matching. We say that a matching is *full* if all vertices in $G(I \cup O)$ are an endpoint of an edge in the matching, and is *partial* otherwise. Clearly, in an $N \times N$ switch, any full matching contains exactly N edges.

3 SERENA

3.1 Overview of SERENA

SERENA is an adaptive algorithm designed to eventually converge to MWM in the sense that the weight of the matching, at any future time slot after the convergence period, is with high probability either equal to or close to that of MWM. This adaptive algorithm is very simple to state: During each time slot t , derive a full matching $R(t)$ from the set of packet arrivals $A(t)$, and then *merge* $R(t)$ with the full matching $S(t-1)$ used in the previous time slot, to arrive at the full matching $S(t)$ to be used for the current time slot t . We next describe these two steps in more details respectively.

3.1.1 Derive $R(t)$ from $A(t)$

In [14], the set of packet arrivals $A(t)$ is modeled to as an *arrival graph*, which we denote also as $A(t)$, as follows: An edge (I_i, O_j) belongs to $A(t)$ if and only if there is a packet arrival¹ to

¹It is assumed in [14] that there is at most one packet arrival to any input port during each time slot.

the corresponding VOQ at time slot t . Note that $A(t)$ is not necessarily a matching, because more than one input ports could have a packet arrival (*i.e.*, edge) destined for the same output port at time slot t . Hence in this case, each output port prunes all such edges incident upon it except the one with the heaviest weight (with ties broken randomly). The pruned graph, denoted as $A'(t)$, is now a matching.

This matching $A'(t)$, which is typically partial, is then randomly populated into a full matching $R(t)$ by pairing the yet unmatched input ports with the yet unmatched output ports in a round-robin manner. Although this POPULATE procedure alone, with the round-robin pairing, has $O(N)$ computational complexity, we will show in [Appendix A](#) that it can be reduced to the computation of prefix sums and solved using the classical parallel algorithm [22] whose time complexity in this context is $O(\log N)$ per port.

3.1.2 Merge $R(t)$ with $S(t-1)$ to obtain $S(t)$

We will show next in [§3.2](#), that through a MERGE procedure, SERENA cherry-picks heavier edges for $S(t)$ from both $R(t)$ with $S(t-1)$, so that the weight of $S(t)$ is larger than or equal to those of both $R(t)$ and $S(t-1)$. This gradual increase of weight over time allows the matching $S(t)$ to converge towards MWM as t increases. The computational complexity of MERGE is however $O(N)$, as will be shown in [§3.2](#). The primary contribution of SERENADE is to reduce this complexity to $O(\log N)$ per input/output port through parallelization.

We color-code and orient edges of $R(t)$ and $S(t-1)$, like in [14], as follows. We color all edges in $R(t)$ red and all edges in $S(t-1)$ green, and hence in the sequel, rename $R(t)$ to S_r (“r” for red) and $S(t-1)$ to S_g (“g” for green) to emphasize the coloring. *We drop the henceforth unnecessary term t here with the implicit understanding that the focus is on the MERGE procedure at time slot t .* We also orient all edges in S_r as pointing from input ports (*i.e.*, I) to output port (*i.e.*, O) and all edges in S_g as pointing from output ports to input ports. We use notations $S_r(I \rightarrow O)$ and $S_g(O \rightarrow I)$ to emphasize this orientation when necessary in the sequel. Finally, we drop the term t from $S(t)$ and denote the final outcome of the MERGE procedure as S . An example pair of thus oriented full matchings $S_r(I \rightarrow O)$ and $S_g(O \rightarrow I)$, over an 8×8 crossbar, are shown in [Figure 2](#).

3.2 The MERGE Procedure

In this section, we describe how the two color-coded oriented full matchings $S_r(I \rightarrow O)$ and $S_g(O \rightarrow I)$ are merged to produce the final full matching S . The MERGE procedure consists of two steps. The first step is to simply union the two full matchings, viewed as two subgraphs of the complete bipartite graph $G(I \cup O)$, into one that we call the *union graph* and denote as $S_r(I \rightarrow O) \cup S_g(O \rightarrow I)$ (or $S_r \cup S_g$ in short). In other words, the union graph $S_r(I \rightarrow O) \cup S_g(O \rightarrow I)$ contains the directed edges in both $S_r(I \rightarrow O)$ and $S_g(O \rightarrow I)$.

It is a mathematical fact that any such union graph can be decomposed into disjoint directed

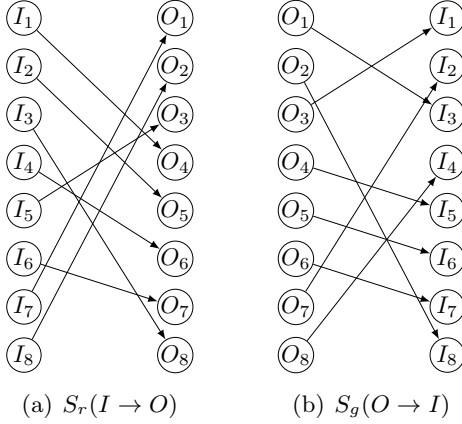


Figure 2: Red matching and green matching.

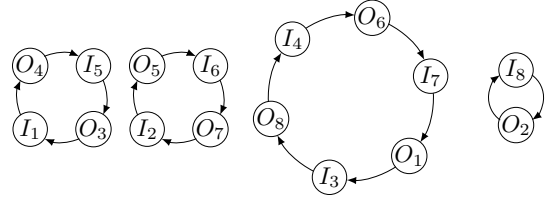


Figure 3: Cycles in $S_r(I \rightarrow O) \cup S_g(O \rightarrow I)$.

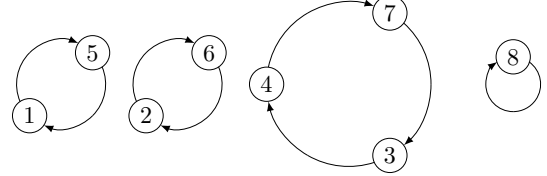


Figure 4: Cycles in $\sigma = \sigma_g^{-1} \circ \sigma_r$.

cycles [14]. Furthermore, each directed cycle, starting from an input port I_i and going back to itself, is an alternating path between a red edge in S_r and a green edge in S_g , and hence contains equal numbers of red edges and green edges. In other words, this cycle consists of a red sub-matching of S_r and a green sub-matching of S_g . Then in the second step, for each directed cycle, the MERGE procedure compares the weight of the red sub-matching (*i.e.*, the total weight of the red edges in the cycle), with that of the green sub-matching, and includes the heavier sub-matching in the final merged matching S .

To illustrate the MERGE procedure by an example, Figure 3 shows the union graph of the two full matchings shown in Figure 2. The union graph contains four disjoint directed cycles that are of lengths 4, 4, 6, and 2 respectively. We do not assign weight to any red or green edge in this example because the cherry-picking of heavier sub-matching is clear from the description above. The standard centralized algorithm for implementing the MERGE procedure is to linearly traverse every cycle once, by following the directed edges in the cycle, to obtain the weights of the green and the red sub-matchings that comprise the cycle [14]. Clearly, this algorithm has a computational complexity of $O(N)$.

3.3 A Combinatorial View of MERGE

So far we have introduced a graph-theoretic view of MERGE, which is adequate for describing MERGE under SERENA. To better describe MERGE under SERENADE however, we introduce a combinatorial view of MERGE, by mapping the two directed full matchings $S_r(I \rightarrow O)$ and $S_g(O \rightarrow I)$ to two permutations σ_r and σ_g^{-1} respectively, as follows. Given a directed full matching $M(I \rightarrow O)$, we map it to a permutation function π over the set $\{1, 2, \dots, N\}$ as follows: $\pi(i) = j$ if and only if input port i is connected to output port j in the matching. By definition, $M(O \rightarrow I)$, the same full matching but with the orientations of all edges reversed, is

mapped to π^{-1} . For example, the full matching $S_r(I \rightarrow O)$ shown in Figure 2(a) is mapped to the permutation $\sigma_r = \begin{pmatrix} 1 & 2 & 3 & 4 & 5 & 6 & 7 & 8 \\ 4 & 5 & 8 & 6 & 3 & 7 & 1 & 2 \end{pmatrix}$. Similarly, $S_g(O \rightarrow I)$ shown in Figure 2(b) is mapped to $\sigma_g^{-1} = \begin{pmatrix} 1 & 2 & 3 & 4 & 5 & 6 & 7 & 8 \\ 3 & 8 & 1 & 5 & 6 & 7 & 2 & 4 \end{pmatrix}$.

We now show that, with the matchings $S_r(I \rightarrow O)$ and $S_g(O \rightarrow I)$ mapped to permutations σ_r and σ_g^{-1} respectively, the MERGE procedure can be very succinctly characterized by a single permutation $\sigma \triangleq \sigma_g^{-1} \circ \sigma_r$, the composition of σ_r and σ_g^{-1} . We do so using the example shown in Figure 2 and Figure 3. It is not hard to check that, in this example, $\sigma \triangleq \sigma_g^{-1} \circ \sigma_r = \begin{pmatrix} 1 & 2 & 3 & 4 & 5 & 6 & 7 & 8 \\ 5 & 6 & 4 & 7 & 1 & 2 & 3 & 8 \end{pmatrix}$. We then decompose this permutation σ into disjoint cycles, which we always can due to Fact 1 below. In this example, $\sigma = (5, 1)(6, 2)(4, 7, 3)(8)$, and its *cycle decomposition graph*, which contains precisely these four combinatorial cycles, is shown in Figure 4.

Fact 1 ([13]) *Any permutation can be written as the product of disjoint cycles.*

Note there is a one-to-one correspondence between the graph cycles (of the union graph $S_r \cup S_g$) shown in Figure 3 and the combinatorial cycles in the cycle decomposition graph (of σ) shown in Figure 4. For example, the graph cycle $I_4 \rightarrow O_6 \rightarrow I_7 \rightarrow O_1 \rightarrow I_3 \rightarrow O_8 \rightarrow I_4$, the third cycle in Figure 3, corresponds to the third combinatorial cycle $(4, 7, 3)$ in Figure 4. Note that two consecutive edges – one belonging to the red matching S_r and the other to the green matching S_g – on the graph cycle “collapse” into an edge on the corresponding combinatorial cycle. For example, two directed edges $(I_4, O_6) (\in S_r)$ and $(O_6, I_7) (\in S_g)$ in Figure 3 collapsed into the directed edge from (input port) 4 to (input port) 7 in Figure 4. Hence each combinatorial cycle subsumes a red sub-matching and a green sub-matching that collapse into it. For example, the combinatorial cycle $(4, 7, 3)$ in Figure 4 subsumes the red sub-matching $\{(I_4, O_6), (I_7, O_1), (I_3, O_8)\}$ and the green sub-matching $\{(O_6, I_7), (O_1, I_3), (O_8, I_4)\}$ in Figure 3. Note also that each vertex on the cycle decomposition graph corresponds to an input port. For example, vertex “4” in Figure 4 corresponds to input port I_4 in Figure 3. Hence, we use the terms “vertex” and “input port” interchangeably in the sequel.

It is important that when two graph edges collapse into a combinatorial edge here, neither graph edge has its weight information forgotten. Hence we assign a green weight $w_g(\cdot)$ and a red weight $w_r(\cdot)$ – to each combinatorial edge e in the cycle decomposition graph – that are equal to the respective weights of the green and the red edges that collapse into e . We also define the green (or red) weight of a combinatorial cycle as the total green (or red) weight of all combinatorial edges on the cycle. Clearly, this green (or red) weight is equal to the weight of the green (or red) sub-matching this cycle subsumes. Under this combinatorial view, the MERGE procedure of SERENA can be stated literally in one sentence: *For each combinatorial cycle in the cycle decomposition graph of σ , we compare its red weight with its green weight, and include in S the corresponding heavier sub-matching.*

3.4 Walks on Cycles

Finally, we introduce the concept of walk on a cycle decomposition graph, which greatly simplifies our descriptions of SERENADE. Recall that a *walk* in a general graph $G(V, E)$ is an ordered sequence of vertices, $v_1 \rightarrow v_2 \rightarrow \dots \rightarrow v_k$ such that $(v_j, v_{j+1}) \in E$ for any $j \in \{1, 2, \dots, k-1\}$; note that a *walk*, unlike a *path*, can traverse a vertex or edge more than once. Clearly, in the cycle decomposition graph of σ , every walk (say starting from a vertex i) circles around a combinatorial cycle (the one that i lies on), and hence necessarily takes the following form: $i \rightarrow \sigma(i) \rightarrow \sigma^2(i) \rightarrow \dots \rightarrow \sigma^m(i)$. For notational convenience, we denote this walk as $i \rightsquigarrow \sigma^m(i)$. For example, with respect to Figure 4, the walk $4 \rightsquigarrow \sigma^8(4)$ represents the $4 \rightarrow 7 \rightarrow 3 \rightarrow 4 \rightarrow 7 \rightarrow 3 \rightarrow 4 \rightarrow 7 \rightarrow 3$ and consists of 8 directed edges on the third cycle in Figure 4.

It will become clear that in most cases, the notation $i \rightsquigarrow \sigma^m(i)$ is sufficiently handy. However, in a few cases, we need a more generalized notation $\sigma^{m_1}(i) \rightsquigarrow \sigma^{m_2}(i)$, where $m_1 < m_2$, and both m_1 and m_2 could be negative. This notation corresponds to the $(m_2 - m_1)$ -edge-long walk $\sigma^{m_1}(i) \rightarrow \sigma^{(m_1+1)}(i) \rightarrow \dots \rightarrow \sigma^{m_2}(i)$.

Now, we define the red and the green weights of a walk as follows. For a walk $i \rightsquigarrow \sigma^m(i)$ in a cycle decomposition graph, we define its red weight, $w_r(i \rightsquigarrow \sigma^m(i))$, as the sum of the red weights of all edges in $i \rightsquigarrow \sigma^m(i)$. Note that if an edge is traversed multiple times in a walk, the red weight of the edge is accounted for multiple times. The green weight of the walk, denoted as $w_g(i \rightsquigarrow \sigma^m(i))$, is similarly defined.

4 The Common Stage of SERENADE

All three SERENADE variants start with an essentially common knowledge-discovery stage that consists of the aforementioned $1 + \log_2 N$ iterations. We refer to this common stage as SERENADE-common and describe it in this section. For ease of presentation (*e.g.*, no need to put floors or ceilings around each occurrence of $\log_2 N$), we have assumed that N is a power of 2 throughout this paper; all SERENADE variants work just as well when N is not.

SERENADE-common uses the standard technique of two-directional exploration with successively doubled distance (hence nicknamed “distance doubling”) in distributed computing [24]. The basic idea of the algorithm is for each vertex i to exchange information, with vertices (± 1) “ σ -hop” away (*i.e.*, $\sigma(i)$ and $\sigma^{-1}(i)$) in the 1st iteration, with vertices (± 2) “ σ -hops” away (*i.e.*, $\sigma^2(i)$ and $\sigma^{-2}(i)$) in the 2nd iteration, with vertices (± 4) “ σ -hops” away (*i.e.*, $\sigma^4(i)$ and $\sigma^{-4}(i)$) in the 3rd iteration, and so on.

Since σ and σ^{-1} are permutations – and so are σ^2 , σ^{-2} , σ^4 , σ^{-4} , and so on – it will become clear that, in each iteration, each of the N vertices is exchanging a message with a distinct vertex. In other words, these N message exchanges are “parallel” to one another, at any moment of time. This “parallelism” has two important implications. First, since these N messages do not “collide” with one another, they can all be transmitted (*i.e.*, switched) simultaneously, by either the main crossbar or an auxiliary crossbar dedicated to the matching

computation. Second, each vertex is doing the same amount of work, namely sending a message and receiving another, at any moment of time. In other words, the communication cost for the matching computation is evenly spread across all vertices.

4.1 Knowledge Sets and Three Ideal Situations

We start with describing the information obtained by SERENADE-common after its $1 + \log_2 N$ iterations; the detailed algorithmic steps in each iteration will be described later in §4.3. After these iterations, each vertex (input port) i obtains the following knowledge sets: $\phi_{k+}^{(i)}$ and $\phi_{k-}^{(i)}$, for $k = 0, 1, 2, \dots, \log_2 N$. Each knowledge set $\phi_{k+}^{(i)}$ contains three quantities concerning the vertex that is 2^k edges “downstream” (*w.r.t.* the direction of the edges), relative to vertex i , in the cycle decomposition graph of σ :

- (1) $\sigma^{2^k}(i)$, the identity of that vertex,
- (2) $w_r(i \rightsquigarrow \sigma^{2^k}(i))$, the red weight of the 2^k -edge-long walk from i to that vertex, and
- (3) $w_g(i \rightsquigarrow \sigma^{2^k}(i))$, the green weight of the walk.

Similarly, each knowledge set $\phi_{k-}^{(i)}$ contains the three quantities concerning the vertex that is 2^k edges “upstream” relative to vertex i , namely $\sigma^{-2^k}(i)$, $w_r(\sigma^{-2^k}(i) \rightsquigarrow i)$, and $w_g(\sigma^{-2^k}(i) \rightsquigarrow i)$. Note that, the knowledge sets of different vertices are different.

Armed with these knowledge sets, a vertex i can determine whether any of the following three ideal situations occurs:

- (1) $i = \sigma^{2^n}(i)$ for some nonnegative integer $n \leq \log_2 N$ (since $\sigma^{2^n}(i) \in \phi_{n+}^{(i)}$);
- (2) $\sigma^{2^n}(i) = \sigma^{2^m}(i)$ for some nonnegative integers $n < m \leq \log_2 N$ (since $\sigma^{2^m}(i) \in \phi_{m+}^{(i)}$);
- (3) $\sigma^{-2^n}(i) = \sigma^{2^m}(i)$ for some nonnegative integers $n < m \leq \log_2 N$ (since $\sigma^{-2^n}(i) \in \phi_{n-}^{(i)}$).

Let l be the length of the cycle to which vertex i belongs. Note that l is the smallest positive integer such that $\sigma^l(i) = i$. The three situations above are considered ideal because, as we will show in Appendix C, whenever one of them occurs, the vertex i – and all other vertices on the same cycle $i \rightsquigarrow \sigma^l(i)$ – know precisely whether $w_g(i \rightsquigarrow \sigma^l(i))$, the green weight of the cycle, or $w_r(i \rightsquigarrow \sigma^l(i))$, the red weight of the cycle, is larger. Therefore, with this knowledge, every vertex on this cycle will select, under SERENADE, the same submatching, as under SERENA. We will show that one or more of the three situations above would happen, if and only if i is on an *ouroboros cycle*, defined next.

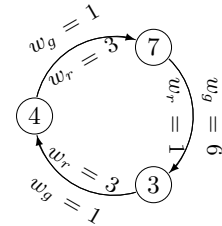


Figure 5: With weights.

Table 1: “Ouroboros statistics” of a uniformly random permutation π .

N	64	128	256	512	1024
\mathcal{O}_N (number of ouroboros numbers <i>w.r.t.</i> N)	36	52	72	99	133
$\mathcal{P}[\pi \text{ is ouroboros}]$	0.342	0.138	0.049	0.019	0.009
$\mathbb{E}_\pi[\text{Broadcast size in O-SERENADE}]$	0.716	1.167	1.695	2.172	2.667
$\mathbb{E}[\text{Binary search length in E-SERENADE} \mid \pi \text{ is non-ouroboros}]$	2.716	3.106	3.600	4.148	4.698

4.2 The Ouroboros Theory

We say a cycle is *ouroboros* if any of the three ideal situations above occurs to one (and necessarily all) of its vertices. Our findings above concerning these three “ouroboros” situations are summarized in the following fact:

Fact 2 *A cycle is ouroboros if and only if its length l is an ouroboros number (w.r.t. N), defined as a positive divisor of a number that takes one of the following three forms:*

- (1) 2^n , for some nonnegative integer $n \leq \lceil \log_2 N \rceil$;
- (2) $2^m - 2^n$, for some nonnegative integers $n < m \leq \lceil \log_2 N \rceil$;
- (3) $2^m + 2^n$, for some nonnegative integers $n < m \leq \lceil \log_2 N \rceil$.

Note that, “ $\lceil \cdot \rceil$ ” can be omitted above, since we have assumed that N is a power of 2. Table 1 shows four different “ouroboros statistics”, when N varies from 64 to 1024. The second row of Table 1 shows \mathcal{O}_N , the number of ouroboros numbers w.r.t. N . \mathcal{O}_N scales roughly as $O(\log^2 N)$ because, in Fact 2, the parameters m and n can take $\frac{1}{2}(\log_2 N)(\log_2(N) - 1)$ possible value combinations.

We say that a permutation σ is ouroboros if all cycles of σ are ouroboros. This case is even better than the three ideal situations above: If σ happens to be ouroboros, then SERENADE algorithm can stop right after these $1 + \log_2 N$ knowledge discovery iterations, and decide on the same matching S as SERENA would. This best-case scenario, however, does not happen very often, especially when N is large (say ≥ 256). More specifically, when σ is a uniform random permutation (*i.e.*, sampled uniformly at random from the set of $N!$ permutation functions over the range $\{1, 2, \dots, N\}$), the third row of Table 1 shows the probability that σ is ouroboros, when N varies from 64 to 1024. For example, this probability is 0.009 when $N = 1,024$. Finally, the last two rows of Table 1 will be explained in §5.2 and §5.4 respectively. The reasons why the uniform random assumption (on σ) is appropriate for explaining the ouroboros statistics are explained in detail in Appendix D.

4.3 SERENADE-common Algorithm

We now describe the $1 + \log_2 N$ iterations of SERENADE-common in detail and explain how these iterations allow every vertex i to concurrently discover its knowledge sets $\{\phi_{k+}^{(i)}\}_{k=0}^{\log_2 N}$ and

$\{\phi_{k-}^{(i)}\}_{k=0}^{\log_2 N}$, for $k = 0, 1, 2, \dots, \log_2 N$.

4.3.1 The 0^{th} Iteration

We start with describing the 0^{th} iteration, the operation of which is slightly different than that of subsequent iterations in that whereas messages are exchanged only between input ports in all subsequent iterations, they are also between input ports and output ports in the 0^{th} iteration. We explain the operation carried out at output port j ; those carried out at any other output port are identical. Suppose output port j is paired with input port i_r in the (red) full matching S_r and with input port i_g in the (green) full matching S_g . The 0^{th} iteration contains two rounds of message exchanges. In the first round, each output port j sends a message to the input port i_g , informing it of the identity i_r and the (red) weight of the edge $i_r \rightarrow j$ in the (red) matching S_r . Note that $\sigma(i_r) = i_g$ by the definition of σ . In the second round, the input port i_g relays the following information to the input port i_r : $w_g(i_r \rightarrow i_g)$ and $w_r(i_r \rightarrow i_g)$. Clearly after this 0^{th} iteration, each input port i learns about the knowledge sets $\phi_{0+}^{(i)}$ and $\phi_{0-}^{(i)}$.

4.3.2 Subsequent Iterations

The subsequent iterations (*i.e.*, iterations $1, 2, \dots, \log_2 N$) are extremely simple when described “inductively” (recursively) as follows. Suppose after iteration $k-1$ (for any $1 \leq k \leq \log_2 N$), every input port i learns the knowledge sets $\phi_{(k-1)+}^{(i)}$ and $\phi_{(k-1)-}^{(i)}$ (*i.e.*, the “induction hypothesis”). We show how every input port i learns the knowledge sets $\phi_{k+}^{(i)}$ and $\phi_{k-}^{(i)}$, after iteration k (*i.e.*, the “inductive step”), the pseudocode of which is presented in [Procedure 1](#). Like iteration 0, iteration k also has two rounds of message exchanges. In the first round, vertex i sends the knowledge set $\phi_{(k-1)+}^{(i)}$, obtained during iteration $k-1$ (by the “induction hypothesis” above), to the upstream vertex $i_U = \sigma^{-2^{k-1}}(i)$ ([line 1](#)). As a result of this round of message exchanges, vertex i will receive from the downstream vertex $i_D = \sigma^{2^{k-1}}(i)$ its knowledge set $\phi_{(k-1)+}^{(i_D)}$ ([line 2](#)), which, as explained earlier, contains the values of $\sigma^{2^{k-1}}(i_D)$, $w_r(i_D \rightsquigarrow \sigma^{2^{k-1}}(i_D))$, and $w_g(i_D \rightsquigarrow \sigma^{2^{k-1}}(i_D))$. Having obtained these three values, vertex i pieces together its knowledge set $\phi_{k+}^{(i)}$ as follows.

$$\begin{aligned} \sigma^{2^k}(i) &\leftarrow \sigma^{2^{k-1}}(i_D) \\ w_r(i \rightsquigarrow \sigma^{2^k}(i)) &\leftarrow w_r(i \rightsquigarrow \sigma^{2^{k-1}}(i)) + w_r(i_D \rightsquigarrow \sigma^{2^{k-1}}(i_D)) \\ w_g(i \rightsquigarrow \sigma^{2^k}(i)) &\leftarrow w_g(i \rightsquigarrow \sigma^{2^{k-1}}(i)) + w_g(i_D \rightsquigarrow \sigma^{2^{k-1}}(i_D)) \end{aligned}$$

Note that vertex i already knows $\phi_{(k-1)+}^{(i)}$ (the “induction hypothesis”), which includes $w_r(i \rightsquigarrow \sigma^{2^{k-1}}(i))$ and $w_g(i \rightsquigarrow \sigma^{2^{k-1}}(i))$.

Similarly, in the second round of message exchanges, i sends $\phi_{(k-1)-}^{(i)}$ to the downstream

vertex i_D (line 3), and at the same time receives $\phi_{(k-1)-}^{(i_U)}$ from the upstream vertex i_U (line 4). The latter knowledge set (*i.e.*, $\phi_{(k-1)-}^{(i_U)}$), combined with the knowledge set $\phi_{(k-1)-}^{(i)}$ that vertex i already knows, allows i to piece together the knowledge set $\phi_{k-}^{(i)}$. Therefore, vertex i obtains $\phi_{k+}^{(i)}$ and $\phi_{k-}^{(i)}$ after the k^{th} iteration, and the “inductive step is proved.” This “inductive step,” combined with the “base case” (the 0^{th} iteration) above, concludes the “induction proof.”

4.3.3 Discussions

Note that, in describing SERENADE-common and all SERENADE variants, we assume that input ports can communicate directly with each other. This is a realistic assumption, because in most real-world switch products, each line card i is full-duplex in the sense the logical input port i and the logical output port i are co-located in the same physical line card i . In this case, for example, an input port i_1 can communicate with another input port i_2 by sending information to output port i_2 , which then relays it to the input port i_2 through the “local bypass”, presumably at little or no communication costs. However, the SERENADE algorithms can also work for the type of switches that do not have such a “local bypass,” by letting an output port to serve as a relay, albeit at twice the communication costs. More precisely, in the example above, the input port i_1 can send the information first to the output port i_1 , which then relays the information to the input port i_2 .

Finally, as shown in line 6 of Procedure 1, i will halt at the earliest time when it finds out the fact that it is on an ouroboros cycle. We will show in Appendix E how i can check for this fact in only $O(1)$ time.

4.4 Complexities of SERENADE-common

The time complexity of SERENADE-common is $1 + \log_2 N$ iterations, and that of each iteration is $O(1)$. The total message complexity of SERENADE-common is $O(N \log N)$ messages, or $O(\log N)$ message per input port, since every vertex needs to send (and receive) two messages during each iteration. This message complexity is smaller than that of iSLIP [27], in which the N input ports need to send, among other things, a total of N^2 bits, indicating whether each of the N^2 VOQs is empty or not, to the switch controller.

5 The SERENADE Variants

In this section, we describe in detail the three variants of SERENADE, namely C-SERENADE (§5.1), O-SERENADE (§5.2), and E-SERENADE (§5.3). Recall that E-SERENADE emulates SERENA exactly, and C-SERENADE and O-SERENADE do so approximately. As explained earlier, if the “union-ed” permutation σ happens to be *ouroboros*, all input ports will find out this fact during or after executing the $1 + \log_2 N$ iterations of SERENADE-common, and

- 1 Send to i_U the knowledge set $\phi_{(k-1)+}^{(i)}$;
- 2 Receive from i_D the knowledge set $\phi_{(k-1)+}^{(i_D)}$;
- 3 Send to i_D the knowledge set $\phi_{(k-1)-}^{(i)}$;
- 4 Receive from i_U the knowledge set $\phi_{(k-1)-}^{(i_U)}$;
- 5 Compute knowledge sets $\phi_k^{(i)}$ and $\phi_{k-}^{(i)}$;
- 6 If i is on an ouroboros cycle (in light of new knowledge $\phi_{k+}^{(i)}$ and $\phi_{k-}^{(i)}$) then halt;

Procedure 1: The k^{th} iteration of SERENADE-common at input port i .

decide on the same “merged” matching S as they would under SERENA (given the same σ). Otherwise, input ports on any *non-ouroboros cycle* do not know for sure at this point, between the red or the green sub-matchings that collapse into the cycle, which one is heavier. The three variants of SERENADE branch off from this point onwards.

Note that the switch has the freedom to choose, for each time slot, which SERENADE variant is to be used. If the switch intends to exercise this freedom, however, the switch controller needs to inform all input ports of its choice at the beginning of the time slot; or all input ports will execute the pre-determined default SERENADE variant. This freedom makes possible the aforementioned hybrid variants such as “mixing 1% E-SERENADE with 99% C-SERENADE,” which we will motivate and elaborate on in §6.

5.1 C-SERENADE

In C-SERENADE, input ports on any such non-ouroboros cycle will each make an individual decision at this point (*i.e.*, without any additional communication and/or computation), according to the following simple rule: Any input port on this non-ouroboros cycle will stay with the green sub-matching (the one used for the previous time slot) and pair again with the output port it paired with in the previous time slot. The logic behind this decision rule is a conservative one: These input ports “stay put” unless they are certain that the alternative is better (*i.e.*, the red sub-matching is heavier). Clearly, the final matching resulting from these individual decisions may or may not be the same as the input ports would decide on under SERENA.

5.2 O-SERENADE

In O-SERENADE, input ports on any such non-ouroboros cycle also have to make a decision based on the same (insufficient) information at hand as in C-SERENADE. Recall every input port i on this cycle knows the green and the red weights of the walk $i \rightsquigarrow \sigma^\eta(i)$, for every η that is an ouroboros number. The *tentative* (to be refined shortly) decision rule of O-SERENADE is

for i to compare the green and the red weights of the longest such walk² $i \rightsquigarrow \sigma^N(i)$, and pick the green or the red edge according to the outcome of this comparison, just like in C-SERENADE.

5.2.1 A Flawed Decision Rule and Its Fix

This tentative decision rule is however flawed because, for two distinct vertices i_1 and i_2 on a non-ouroboros cycle, it is possible that $w_g(i_1 \rightsquigarrow \sigma^N(i_1)) \geq w_r(i_1 \rightsquigarrow \sigma^N(i_1))$ (so i_1 picks the green edge) yet $w_g(i_2 \rightsquigarrow \sigma^N(i_2)) < w_r(i_2 \rightsquigarrow \sigma^N(i_2))$ (so i_2 picks the red edge). In other words, i_1 and i_2 have *inconsistent local views* as to which sub-matching is heavier. It is not hard to check that, in this case, at least two distinct input ports (not necessarily i_1 and/or i_2) on this non-ouroboros cycle would be paired with the same output port, resulting in a configuration collision.

Figure 5 shows an example of such inconsistent local views: $w_g(3 \rightsquigarrow \sigma^8(3)) = 18 < 20 = w_r(3 \rightsquigarrow \sigma^8(3))$ (vertex 3's local view) and $w_g(7 \rightsquigarrow \sigma^8(7)) = 23 > 18 = w_r(7 \rightsquigarrow \sigma^8(7))$ (vertex 7's local view). Although the inconsistent local views here do not result in a configuration collision because the cycle (3, 4, 7) is ouroboros (3 is an ouroboros number), they would in a non-ouroboros cycle. Note that, as mentioned earlier, since the smallest non-ouroboros number is 19 (when $N \geq 64$ and is a power of 2), a more qualified example involving a non-ouroboros cycle would be unnecessarily large and complex to plot here.

O-SERENADE fixes this flaw by letting a designated leader vertex – which we denote as \mathcal{L}_0 – on this cycle to make such a decision for all vertices on this cycle, based on its local view (of $w_r(\mathcal{L}_0 \rightsquigarrow \sigma^N(\mathcal{L}_0))$ vs. $w_g(\mathcal{L}_0 \rightsquigarrow \sigma^N(\mathcal{L}_0))$). This leader \mathcal{L}_0 is decided through a distributed leader election [24] by the vertices on this cycle. Although distributed leader election is general a relatively expensive operation [3, 24], we will show shortly in §5.2.2 that leader election in O-SERENADE on each non-ouroboros cycle can be seamlessly embedded into the $1 + \log_2 N$ iterations of SERENADE-common, and leader elections on distinct non-ouroboros cycles can be computed in parallel. Once the leader of a non-ouroboros cycle is decided, the leader \mathcal{L}_0 informs the switch controller of its decision on whether to choose the green or the red sub-matching. The switching controller then broadcasts a list of leaders, one for each non-ouroboros cycle, and their decisions to all N vertices. Since each vertex on an ouroboros cycle knows the identity of its leader, as we will “prove” in §5.2.2, it will follow the decision made by its leader in choosing between the red and the green edges.

The size of this broadcast, equal to the number of *non-ouroboros* cycles in a permutation, is small (with overwhelming probability), as shown in the fourth row of Table 1 for a uniform random permutation (same for other random permutations as observed in our simulation results). For example, even when $N = 1,024$, the average broadcast size is only 2.667. Intuitively, this is because, for this number to be large, there has to be many short cycles, but all short cycles (up to length 22 when $N = 1,024$) are ouroboros.

²Recall that we assume N is a power of 2, so N is an ouroboros number.

This solution solves the *decision consistency problem* of O-SERENADE: It guarantees that all vertices on a non-ouroboros cycle make a consistent decision (by picking the same sub-matching). However, like in C-SERENADE, there is no guarantee that the final decision results in the heavier sub-matching of the cycle being chosen, so O-SERENADE also emulates SERENA only approximately. However, empirically the heavier sub-matching is chosen most of the time, as we will show and explain why in §7.2. An alternative solution used in [30] to this *decision consistency problem* is described and compared with in Appendix F.

5.2.2 Leader Election

In this section, we describe the leader election process in O-SERENADE. As explained earlier, O-SERENADE does not have to pay much extra for running this leader election: The election process can be seamlessly embedded into the $1 + \log_2 N$ knowledge-discovery iterations of SERENADE-common. More specifically, O-SERENADE only needs to add, in each iteration, to one of the two messages transmitted in SERENADE-common, a $\log_2 N$ -bit-long leadership knowledge field.

Now we describe how this embedding is performed, in an arbitrary non-ouroboros cycle, focusing on the actions of a vertex i that belongs to this cycle. We follow the standard practice [31] of making the vertex with the smallest identity (an integer between 1 and N) on this cycle the leader. Recall that in SERENADE-common, after each (say k^{th}) iteration, vertex i learns $\phi_{k-}^{(i)}$, which contains the identities of the vertex $\sigma^{-2^k}(i)$ that is “ 2^k hops away” from it on the cycle, and the red and the green weights of the walk $\sigma^{-2^k}(i) \rightsquigarrow i$. Our goal is to augment this k^{th} iteration to learn the vertex with the smallest identity on this walk $\sigma^{-2^k}(i) \rightsquigarrow i$, which we denote as $\mathcal{L}(\sigma^{-2^k}(i) \rightsquigarrow i)$ and call a level- k “precinct leader.” This way, after the $(\log_2 N)^{\text{th}}$ iteration, input port i learns the identity of the level- $(\log_2 N)$ precinct leader $\mathcal{L}(\sigma^{-N}(i) \rightsquigarrow i)$, which must be \mathcal{L}_0 , the leader of the entire cycle, because the length of this cycle is no larger than N , the length of the precinct (walk) $\sigma^{-N}(i) \rightsquigarrow i$.

Like in SERENADE-common, we explain this augmentation “inductively.” The case of $k = 0$ is trivial: Each vertex i considers the one with smaller identity between itself and $\sigma^{-1}(i)$ to be the leader of its respective level-0 precinct. We claim that after iteration $k - 1$, every input port i gets two things done (This claim is “the induction hypothesis”). First, i learns the identity of $\mathcal{L}(\sigma^{-(2^{k-1})}(i) \rightsquigarrow i)$, the leader of the level- $(k - 1)$ precinct leader right-ended at i (Part I of the claim). Second, i receives, from $i_U = \sigma^{-(2^{k-1})}(i)$, the vertex 2^{k-1} hops upstream, its level- $(k - 1)$ precinct leader information (Part II of the claim). However, the union of these two level- $(k - 1)$ precincts $\mathcal{L}(\sigma^{-(2^{k-1})}(i) \rightsquigarrow i)$ and $\mathcal{L}(\sigma^{-(2^{k-1})}(i_U) \rightsquigarrow i_U)$ is precisely the level- k precinct $\mathcal{L}(\sigma^{-2^k}(i) \rightsquigarrow i)$. Hence, in iteration k , input port i simply computes $\mathcal{L}(\sigma^{-2^k}(i) \rightsquigarrow i) \leftarrow \min \{ \mathcal{L}(\sigma^{-(2^{k-1})}(i_U) \rightsquigarrow i_U), \mathcal{L}(\sigma^{-(2^{k-1})}(i) \rightsquigarrow i) \}$, so part I of the above claim is fulfilled; this local computation is added to Procedure 1 as “line 5.5”. In addition, (each) vertex i sends the information $\mathcal{L}(\sigma^{-(2^{k-1})}(i) \rightsquigarrow i)$ downstream to $i_D = \sigma^{2^{k-1}}(i)$, so part II of

the above claim is fulfilled; this information is appended to the message that i sends to i_D in [line 3 of Procedure 1](#) and hence does not require a separate message exchange. Therefore, the “inductive step is proved”.

Note that the leadership information has to be included in the messages from the 0^{th} iteration onwards, if the switch intends to execute O-SERENADE in this time slot. This is the reason why the switch controller is required to declare this intention at the beginning of the time slot (mentioned in [§5](#)).

5.3 E-SERENADE

Whereas in C-SERENADE and O-SERENADE, each non-ouroboros cycle picks a sub-matching, which may or may not be the heavier one, right after the SERENADE-common’s $1 + \log_2 N$ iterations, in E-SERENADE, vertices on each non-ouroboros cycle execute an additional distributed algorithm to find out *exactly* which sub-matching is heavier. Like O-SERENADE, E-SERENADE requires that all $1 + \log_2 N$ SERENADE-common iterations be augmented with leader election. Recall that, for a vertex i on a non-ouroboros cycle, the “final product” of the leader election process is $\mathcal{L}(\sigma^{-N}(i) \rightsquigarrow i)$, the leader of the level- $(\log_2 N)$ precinct right-ended at i , which is also \mathcal{L}_0 , the leader of the entire cycle. However, during this process, i also obtains, as “intermediate products”, the identities of the leaders of level- k precincts right-ended at i , *i.e.*, $\mathcal{L}(\sigma^{-2^k}(i) \rightsquigarrow i)$ for $k = 0, 1, \dots, \log_2(N) - 1$. We will show next that whereas in O-SERENADE only the “final product” is used, in E-SERENADE, all “intermediate products” will also be put to full use.

5.3.1 Distributed Binary Search

It suffices to describe this distributed algorithm on an arbitrary non-ouroboros cycle, since every non-ouroboros cycle runs an (distinct) instance of the same algorithm. Hence, without loss of generality, we assume that \mathcal{L}_0 is the leader of, and i a vertex on, this non-ouroboros cycle. The objective of this distributed algorithm is to search for a *repetition* (*i.e.*, other than its first occurrence as the starting point of the walk) of its leader \mathcal{L}_0 along the walk $\mathcal{L}_0 \rightsquigarrow \sigma^N(\mathcal{L}_0)$, the level- $(\log_2 N)$ precinct right-ended at $\sigma^N(\mathcal{L}_0)$; this repetition must exist because N , the length of the walk $\mathcal{L}_0 \rightsquigarrow \sigma^N(\mathcal{L}_0)$, is no smaller than the length of this cycle. To this end, vertices on this non-ouroboros cycle perform a distributed binary search – guided by the aforementioned “intermediate” and “final products” each vertex obtains through the leader election process – as follows.

This binary search is initiated by the vertex $\sigma^N(\mathcal{L}_0)$, who learns “who herself is” (*i.e.*, that herself is $\sigma^N(\mathcal{L}_0)$) during the last iteration of SERENADE-common; in other words, the initial *search administrator* is $\sigma^N(\mathcal{L}_0)$. The initial *search interval* is the entire walk $\mathcal{L}_0 \rightsquigarrow \sigma^N(\mathcal{L}_0)$, also the level- $(\log_2 N)$ precinct right-ended at $\sigma^N(\mathcal{L}_0)$. $\sigma^N(\mathcal{L}_0)$ first checks whether there is a repetition of \mathcal{L}_0 in the right half of the search interval (*i.e.*, the walk $\sigma^{-N/2}(i) \rightsquigarrow i$) by checking

whether³ $\mathcal{L}(\sigma^{N/2}(\mathcal{L}_0) \rightsquigarrow \sigma^N(\mathcal{L}_0))$ is equal to \mathcal{L}_0 . If so, the search administrator $\sigma^N(\mathcal{L}_0)$ carries on this binary search in the right half of the search interval. Otherwise, the “middle point” of the search interval $\sigma^{N/2}(\mathcal{L}_0)$ becomes the new search administrator and carries on this binary search in the left half.

5.3.2 “Bookkeeping” the Weight Information

This way, with each step of this binary search, the search interval is halved (and becomes a precinct that is one level lower), and if needed, a different vertex that is at least twice as close to the target becomes the new search administrator. We will provide the details of this binary search algorithm later in §5.3.3. We highlight here, however, the following important invariant this binary search algorithm maintains. Whenever a vertex (say $\sigma^u(\mathcal{L}_0)$) becomes the new search administrator, the search algorithm maintains the red and the green weights of the walk $\mathcal{L}_0 \rightsquigarrow \sigma^u(\mathcal{L}_0)$. This way, when the search administrator finally reaches a repetition of \mathcal{L}_0 (say $\sigma^v(\mathcal{L}_0)$), we also obtain the red and green weights of the walk $\mathcal{L}_0 \rightsquigarrow \sigma^v(\mathcal{L}_0)$. Comparing these two weights allows us to tell precisely whether the green weight or the red weight of the cycle is heavier because, the walk $\mathcal{L}_0 \rightsquigarrow \sigma^v(\mathcal{L}_0)$ coils around the cycle for an integer number of times (since the endpoint $\sigma^v(\mathcal{L}_0)$ is a repetition of the starting point \mathcal{L}_0).

Like in O-SERENADE, the leader of each non-ouroboros cycle needs to “register” its identity with the switch controller, at the end of the leader-election-augmented SERENADE-common. However, unlike in O-SERENADE, the leader informs the switch controller, of its determination (as to which sub-matching is heavier) only after the distributed binary search completes on the non-ouroboros cycle. The switch controller then broadcasts the aforementioned list of leaders and their determinations to all vertices only after hearing from all “registered” leaders. The “registration” process is important for minimizing the average additional delay of E-SERENADE because, without it, the switch would have to conservatively wait the maximum amount of time it would possibly take for the distributed binary search process to complete on every non-ouroboros cycle.

5.3.3 Binary Search for a Repetition of \mathcal{L}_0

In this section, we describe in detail the distributed binary search algorithm used in E-SERENADE by vertices of a non-ouroboros cycle to find a repetition of its leader (say \mathcal{L}_0) along the walk $\mathcal{L}_0 \rightsquigarrow \sigma^N(\mathcal{L}_0)$. [Procedure 2](#) captures the action of a vertex i along the search path (*i.e.*, vertex i is the search administrator at this moment). Its computational task is to search for and “close in on” a repetition of \mathcal{L}_0 in the search interval $\sigma^{-2^k}(i) \rightsquigarrow i$, the level- k (where k is the 2^{nd} argument of *BinarySearch* in [line 1](#)) precinct right-ended at i . It does so as follows. Vertex

³The identity of $\mathcal{L}(\sigma^{N/2}(\mathcal{L}_0) \rightsquigarrow \sigma^N(\mathcal{L}_0))$, the leader of the level- $(\log_2(N) - 1)$ precinct right-ended at $\sigma^N(\mathcal{L}_0)$, is known to $\sigma^N(\mathcal{L}_0)$, since it is one of the aforementioned “intermediate products” $\sigma^N(\mathcal{L}_0)$ learns through the leader election process.

```

1 Procedure BinarySearch( $i, k, w_g, w_r$ )
2   If  $i$  (self) is  $\mathcal{L}_0$  then halt;
3   if  $\sigma^{(-2^{k-1})}(i) = \mathcal{L}_0$  then
4      $w_g \leftarrow w_g - w_g(\sigma^{(-2^{k-1})}(i) \rightsquigarrow i)$ ;
5      $w_r \leftarrow w_r - w_r(\sigma^{(-2^{k-1})}(i) \rightsquigarrow i)$ ;
6     BinarySearch( $\mathcal{L}_0, k-1, w_g, w_r$ );
7   else
8     if  $\mathcal{L}_0 = \mathcal{L}(\sigma^{(-2^{k-1})}(i) \rightsquigarrow i)$  then
9       | BinarySearch( $i, k-1, w_g, w_r$ );
10    else
11       $w_g \leftarrow w_g - w_g(\sigma^{(-2^{k-1})}(i) \rightsquigarrow i)$ ;
12       $w_r \leftarrow w_r - w_r(\sigma^{(-2^{k-1})}(i) \rightsquigarrow i)$ ;
13      BinarySearch( $\sigma^{(-2^{k-1})}(i), k-1, w_g, w_r$ );

```

Procedure 2: Binary search at input port i .

i first checks (in lines 2 and 3) whether itself or $\sigma^{(-2^{k-1})}(i)$, the middle point of the search interval, is a repetition of \mathcal{L}_0 . If so, the entire mission is accomplished so the search ends.

Otherwise, vertex i checks whether there is a repetition of \mathcal{L}_0 along the walk $\sigma^{(-2^{k-1})}(i) \rightsquigarrow i$ (the right half of the current search interval), which is precisely the level- $(k-1)$ precinct right-ended at i . Hence this is equivalent to check (line 8), whether $\mathcal{L}(\sigma^{(-2^{k-1})}(i) \rightsquigarrow i)$, the leader of this precinct (known to vertex i as an intermediate product of the leader election) is equal to the cycle leader \mathcal{L}_0 . If the answer is yes, vertex i continues to search (*i.e.*, the search administrator remains to be vertex i) in this right half (line 9). Otherwise, vertex i passes the “baton” to the middle point $\sigma^{(-2^{k-1})}(i)$ (the new search administrator), which will continue the search in the walk $\sigma^{(-2^k)}(i) \rightsquigarrow \sigma^{(-2^{k-1})}(i)$, the left half of the current search interval (line 13).

When vertex i becomes the new search administrator, it also receives (from the previous search administrator) w_g and w_r , the aforementioned green and red weights of the walk from \mathcal{L}_0 to the new search administrator (3^{rd} and 4^{th} arguments of Procedure 2 in line 1). Before passing the “baton”, vertex i makes the aforementioned (in §5.3.2) modifications to w_g and w_r so that they are now equal to the green and red weights of the walk from \mathcal{L}_0 to the new search administrator $\sigma^{(-2^{k-1})}(i)$.

Note that we write Procedure 2 as a “recursive program” only to make it as succinct as possible; it is not a recursive program and does not reflect the computational complexity of the search. More specifically, the “recursive call” *BinarySearch*(i, k, w_g, w_r) in Procedure 2 is simply to send a message to vertex i containing these arguments, and there is no need for i to send itself a message when making a “recursive call” to itself (*e.g.*, in line 9). In fact, vertex i can identify

the smallest (*i.e.*, lowest-level) precinct right-ended at i that contains \mathcal{L}_0 , without performing any additional computation, by recording this information during the leader election process, as follows. During the iterations of SERENADE-common augmented with leader election, vertex i remembers the identity of the presumptive leader (given all the information available at the time) and *when* (*i.e.*, during which iteration) this presumptive leader was installed. Recall that at the end of the k^{th} iteration, vertex i learns the identity of the level- k precinct leader right-ended at vertex i . If this identity is smaller than that of the presumptive leader, the former is installed as the new presumptive leader, and its “installation time” is k . This way, every vertex i learns when \mathcal{L}_0 was installed at the presumptive leader, which is the same as the smallest (*i.e.*, lowest-level) precinct right-ended at i that contains \mathcal{L}_0 .

5.4 Complexity of SERENADE Variants

Table 2: Complexities of SERENADE variants.

	Time complexity	Message complexity per vertex
C-SERENADE	$1 + \log_2 N$	$O(\log N)$
O-SERENADE	$1 + \log_2 N$	$O(\log N)$
E-SERENADE	$\approx 1.5 \log_2 N$	$O(\log N)$

Recall (from §4.4) that SERENADE-common has a time complexity of $1 + \log_2 N$ iterations and a total message complexity of $O(N \log N)$ messages, or $O(\log N)$ messages per input port. In this section, we analyze the time and the total message complexities, *in addition to* those of SERENADE-common, of the three SERENADE variants. Table 2 summarizes their complexities.

C-SERENADE and O-SERENADE. C-SERENADE incurs no additional time and message complexities, as it makes a conservative decision right after SERENADE-common’s $1 + \log_2 N$ iterations. Almost the same can be said about O-SERENADE: The total message complexity involved for the leaders of non-ouroboros cycles to report their respective decisions to the switch controller is nearly a constant (see the third paragraph of §5.2.1), plus a broadcast of these decisions; the additional time complexity is just 1 iteration. However, since O-SERENADE requires leader election, every message exchange in SERENADE-common has to include the identity of a precinct leader, which increases a length of each message by $\log_2 N$ bits. We will show in §7.2 that this is a modest cost to pay for the significantly better delay performance than that of C-SERENADE.

E-SERENADE. In E-SERENADE, due to the binary nature of the search (for a repetition of its leader on every non-ouroboros cycle), the additional time complexity, in the worst case, is upper-bounded by $\lceil \log_2 \eta \rceil$ ($\leq \log_2 N$), where η is the length of the longest non-ouroboros cycle.

The average additional time complexity, however, is much smaller than $\log_2 N$, for the following reason. It takes practically no time for a search administrator i to narrow the search interval to the smallest precinct right-ended at i , since i can remember this information (when the vertex with the smallest identity among those “seen” so far first becomes a precinct leader) during the SERENADE-common iterations. Hence, a unit of time complexity is incurred only when the search administrator has to move from one vertex to another, which happens often much less than $\lceil \log_2 \eta' \rceil$ on a non-ouroboros cycle of length η' . For example, the average time complexity as a function of N , when σ is a uniform random permutation, is shown in the last row of [Table 1](#). It is roughly between $0.46 \log_2 N$ and $0.48 \log_2 N$, for these values of N . Therefore, we consider E-SERENADE to be 1.5 times more expensive, in terms of time complexity, than C-SERENADE and O-SERENADE.

As shown in [§5.3.3](#), during the binary search process, on each non-ouroboros cycle a message is transmitted ([line 13](#) in [Procedure 2](#)) only when the search administrator moves from one vertex to another. Since each vertex receives and transmits at most one message each during the binary search process, the total additional message complexity of E-SERENADE, in the worst-case, is bounded by $O(N)$. This message complexity is small compared to that of SERENADE-common, which is $O(N \log N)$. In fact, it can be shown that the average additional message complexity is bounded by $O(\log^2 N)$.

6 Hybrid SERENADE Schemes

It is always desirable for a crossbar scheduling algorithm to achieve 100% throughput in the following sense: The N^2 -dimensional VOQ length vector is *stable* – *i.e.*, is an ergodic Markov chain with finite first moment – under any admissible *i.i.d.* traffic arrival process. Although both C-SERENADE and O-SERENADE can empirically achieve 100% throughput under the four standard traffic patterns (see [§7.1](#)), we are so far not able to prove that they can do so under all traffic patterns, and we have explained in [Appendix H.2.3](#) why it is difficult to obtain this proof. However, the good news is that E-SERENADE not only provably achieves 100% throughput itself by exactly emulating SERENA, but also can serve as a “stabilizer” to C-SERENADE and O-SERENADE, when a tiny percent (say α) of E-SERENADE is probabilistically “mixed” with them. The following two hybrid SERENADE schemes, namely SC-SERENADE and SO-SERENADE, are the resulting stabilized products.

SC-SERENADE (Stabilized C-SERENADE). At the beginning of each time slot, the switch controller flips a biased coin that lands on head with a tiny probability α (say $\alpha = 0.01$) and on tail with probability $1 - \alpha$. The controller runs E-SERENADE, if the outcome is head, and C-SERENADE otherwise. We will prove in [Appendix H](#) that SC-SERENADE can achieve 100% throughput, with any $\alpha > 0$.

SO-SERENADE (Stabilized O-SERENADE). Like in SC-SERENADE, in each time slot, the switch controller runs E-SERENADE with probability α and a slightly modified O-

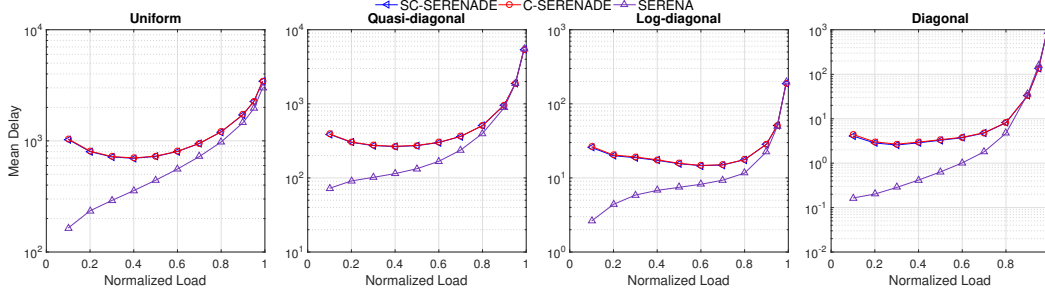


Figure 6: Mean delays of C-SERENADE, SC-SERENADE and SERENA under the 4 traffic load matrices.

SERENADE with probability $1-\alpha$. The modification, which we call Conservative-if-OverWeight (COW), is that, vertices of a non-ouroboros cycle would use the decision rule of C-SERENADE (*i.e.*, pick the sub-matching used in the previous time slot), if any edge on the cycle is “overweight” (*i.e.*, has a weight larger than a high threshold, such as 10,000). We will show in [Appendix H](#) that, with this COW modification, it is straightforward to prove that SO-SERENADE can achieve 100% throughput, with any $\alpha > 0$. The COW modification is simple to implement and has negligible additional overhead: add a single bit to every SERENADE-common message indicating whether any edge along the corresponding walk is found to be overweight.

Since as explained earlier E-SERENADE is only roughly 1.5 times, in terms of both time and message complexities, as expensive as O-SERENADE, SC-SERENADE and SO-SERENADE are only slightly more expensive (say between 1.005 and 1.01 times more expensive when $\alpha = 0.01$) than C-SERENADE and O-SERENADE respectively, when α is tiny. This is undoubtedly a modest cost to pay for the provable stability guarantees SC-SERENADE and SO-SERENADE afford us.

7 Performance Evaluation

In this section, we evaluate, through simulations, the throughput and the delay performances of C-SERENADE and O-SERENADE⁵, and their stabilized variants SC-SERENADE and SO-SERENADE, under various load conditions and traffic patterns to be specified in [§7.1](#). We also compare their delay performances with that of SERENA [\[14\]](#), the algorithm they try to approximate. The evaluation results, to be presented in [§7.2](#), show conclusively that C-SERENADE and O-SERENADE trade either slight or no degradation of delay performances for significant reduction in time complexities.

⁵There is no need to evaluate that of E-SERENADE, which exactly emulates SERENA.

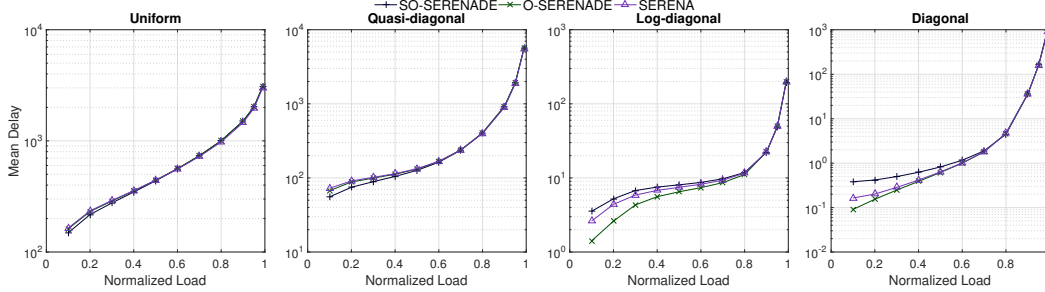


Figure 7: Mean delays of O-SERENADE, SO-SERENADE and SERENA under the 4 traffic load matrices.

7.1 Simulation Setup

In all our simulations, we set the number of input/output ports N to 64. We have however also investigated how the mean delay performances of these scheduling algorithms scale with respect to N , and the findings are reported in [Appendix I.2](#). To measure throughput and delay accurately, we assume each VOQ has an infinite buffer size and hence there is no packet drop at any input port. Every simulation run lasts $30,000 \times N^2$ ($\approx 1.23 \times 10^8$) time slots. This duration is chosen so that every simulation run enters the steady state after a tiny fraction of this duration and stays there for the rest. The throughput and delay measurements are taken after the simulation run enters the steady state.

Like in [14], we assume, in the following simulations, that the traffic arrival processes to different input ports are mutually independent, and each such arrival process is *i.i.d.* Bernoulli (*i.e.*, at any given input port, a packet arrives with a constant probability $\rho \in (0, 1)$ during each time slot). The following 4 standard types of load matrices (*i.e.*, traffic patterns) are used to generate the workloads of the switch:

- (1) *Uniform*: packets arriving at any input port go to each output port with probability $\frac{1}{N}$.
- (2) *Quasi-diagonal*: packets arriving at input port i go to output port $j = i$ with probability $\frac{1}{2}$ and go to any other output port with probability $\frac{1}{2(N-1)}$.
- (3) *Log-diagonal*: packets arriving at input port i go to output port $j = i$ with probability $\frac{2^{(N-1)}}{2^N - 1}$ and go to any other output port j with probability equal $\frac{1}{2}$ of the probability of output port $j - 1$ (note: output port 0 equals output port N).
- (4) *Diagonal*: packets arriving at input port i go to output port $j = i$ with probability $\frac{2}{3}$, or go to output port $(i \bmod N) + 1$ with probability $\frac{1}{3}$.

The load matrices are listed in order of how skewed the traffic volumes to different output ports are: from uniform being the least skewed, to diagonal being the most skewed. Finally, we emphasize that, every non-zero diagonal element (*i.e.*, traffic from an input port i and an output port i), in every traffic matrix we simulated on, is actually *switched* by the crossbar

and consumes just as much switching resources per packet as other traffic matrix elements, and never “evaporates” over the “local bypass” (see §4.3.3) that may exist between the input port i and the output port i .

7.2 Simulation Results

In this section, we present only simulation results of SERENA and all SERENADE variants under (non-bursty) Bernoulli i.i.d. arrival processes described above. We have also simulated them under busy ON-OFF arrival processes. Those simulation results, which show that all SERENADE variants perform as well as SERENA under heavy bursty traffic, will be shown in [Appendix I.1](#).

7.2.1 Throughput Performance

First of all, our simulation results show that both C-SERENADE and O-SERENADE (without the COW modification) can empirically achieve 100% throughput under all 4 traffic load matrices and *i.i.d.* Bernoulli traffic arrivals: The VOQ lengths remain stable under an offered load of 0.99 in all these simulations. Both SERENADE’s also do so under bursty traffic arrivals, as shown in [Appendix I.1](#).

7.2.2 Delay Performance

Now we shift our focus to the delay performances of C-SERENADE and O-SERENADE, and their stabilized variants SC-SERENADE and SO-SERENADE. We compare their delay performances only with that of SERENA, because the merits of SERENA (*e.g.*, superb complexity-performance tradeoff) were thoroughly established in [14]. We refer readers to [14] for detailed performance (throughput and delay) comparisons between SERENA and some other crossbar scheduling algorithms such as iSLIP [27], iLQF [26], and MWM [28].

C-SERENADE vs. SERENA. We first compare C-SERENADE, SC-SERENADE, and SERENA. We set $\alpha = 0.01$ in SC-SERENADE (*i.e.*, mix 1% of E-SERENADE with C-SERENADE). [Figure 6](#) shows the mean delays of the three algorithms under the 4 traffic load matrices above respectively. Each subfigure shows how the mean delays (on a *log scale* along the y-axis) vary with different offered loads (along the x-axis). We can make two observations from [Figure 6](#). First, [Figure 6](#) clearly shows that the delay performances of C-SERENADE and SC-SERENADE are almost the same: Their curves almost completely overlap with each other. Hence, we discuss only C-SERENADE in further comparisons with SERENA.

Second, [Figure 6](#) shows that, under all 4 traffic load matrices, the delay performance of C-SERENADE is worse than that of SERENA when the traffic load is low, but their delay performances converge when the traffic load is high. Our interpretation of this observation is as follows. C-SERENADE in general should perform worse (in mean delay) than SERENA, due to its conservative decision rule of sticking to the old (green) sub-matching on any non-ouroboros

cycle, even when it is not as heavy as the new (red) sub-matching. However, the “damage” of being conservative to the delay performance is much larger when the traffic is light – and VOQ lengths are small – for the following reason. The old sub-matching “loses weight” at a high relative (to its current weight) rate, and some of its VOQs (edges) could even become empty (*i.e.*, have weight 0), whereas the new sub-matching can “gain weight” at a high relative rate. This damage becomes tiny when the traffic is very heavy – and VOQ lengths are long – because once C-SERENADE settles in a very heavy matching, the matching (and its sub-matchings) will remain very heavy, relative to both its current weight and those of other “rising star” (in weight) matchings, for quite a while.

O-SERENADE vs. SERENA. Next, we compare the mean delay performances of O-SERENADE and SO-SERENADE with that of SERENA. Again this (standalone) O-SERENADE is without the COW modification, but the O-SERENADE part of SO-SERENADE is and the overweight threshold (for any VOQ/edge) is set to 10,000 packets. Again we set $\alpha = 0.01$ in SO-SERENADE (*i.e.*, run E-SERENADE 1% of the time at random). Figure 7 shows the mean delays of the three algorithms under the 4 traffic load matrices above respectively. Each subfigure shows how the mean delays (on a *log scale* along the y-axis) vary with different offered loads (along the x-axis). Figure 7 shows that overall the three algorithms perform similarly under all 4 traffic load matrices and all load factors. Upon observing these simulation results, our interpretation was that the decisions made by O-SERENADE agree with the ground truth (*i.e.*, which sub-matching is indeed heavier on a non-ouroboros cycle) most of time. This interpretation was later confirmed by further simulations: They agree in between 90.57% and 99.99% of the instances.

Perhaps surprisingly, Figure 7 also shows that O-SERENADE performs slightly better than SO-SERENADE and SERENA when the traffic load is low (say < 0.4), especially under log-diagonal and diagonal traffic load matrices. Our interpretation of this observation is as follows. It is not hard to verify that decisions made by O-SERENADE can disagree with the ground truth, with a non-negligible probability, only when the total green and the total red weights of a non-ouroboros cycle are very close to one another. However, in such cases, picking the wrong sub-matchings (*i.e.*, disagreeing with the ground truth) causes almost no damages. Furthermore, we speculate that it may even help O-SERENADE jump out of a local maximum (*i.e.*, have the effect of simulated annealing) and converge more quickly to a global maximum weighted matching, thus resulting in even better delay performance.

C-SERENADE vs. O-SERENADE. We prefer O-SERENADE over C-SERENADE for two reasons. First, O-SERENADE performs either the same as or slightly better than SERENA, under all 4 traffic load matrices and all load factors; the same cannot be said about C-SERENADE, as shown earlier. Second, O-SERENADE is only slightly more expensive, in terms of both time and message complexities, than C-SERENADE.

8 Related Work

In the interest of space, we provide only a brief survey of the prior art that is directly related to our work. Since SERENADE parallelizes SERENA, which computes approximate Maximum Weight Matching (MWM), we focus mostly on the following two categories: (1) parallel or distributed algorithms for exact or approximate MWM computation with applications to crossbar scheduling (in §8.1) and (2) distributed matching algorithms with applications to transmission scheduling in wireless networks (in §8.2). In particular, we will keep to a minimum the comparisons between SERENA and other sequential crossbar scheduling algorithms proposed before SERENA, of which a fine job was already done in [14].

A few *sequential* crossbar scheduling algorithms were proposed recently [17, 41]. However, none of these algorithms beats SERENA in both (delay and throughput) performance and computational complexity under the standard problem setting (*e.g.*, fixed packet size). A template that can be instantiated into a family of throughput-optimal algorithms for scheduling crossbar or wireless transmission, and a unified framework for proving the throughput-optimality of all these algorithms were proposed in [35, 36]. In [35, 36], the only crossbar scheduling algorithm that results from this template is the instantiation of a BP-based MWM algorithm [5], which has a message and time complexity of $O(N)$ per port. Recently, an “add-on” algorithm called Queue-Proportional Sampling (QPS) was proposed in [15] that can be used to augment, and boost the delay performance of, SERENA [14]. However, the resulting QPS-SERENA has the same $O(N)$ time complexity as SERENA.

8.1 Parallel/Distributed MWM Algorithms

As mentioned earlier, MWM is the ideal crossbar scheduling policy, but its most efficient algorithmic implementation [11] has a prohibitively high computational complexity of $O(N^3)$. This dilemma has motivated the development of a few parallel or distributed algorithms that, by distributing this computational cost across multiple processors (nodes), bring down the per-node computational complexity.

The most representative among them are [2, 4, 5, 12]. A parallel algorithm with a sub-linear per-node computational complexity of $O(\sqrt{N} \log^2 N)$ was proposed in [12] for computing MWM exactly in a bipartite graph. However, this algorithm requires the use of $O(N^3)$ processors. Another two [4, 5] belong to the family of distributed iterative algorithms based on belief-propagation (BP). In this family, the input ports engage in multiple iterations of message exchanges with the output ports to learn enough information about the lengths of all N^2 VOQs so that each input port can decide on a distinct output port to match with. The resulting matching either is, or is close to, the MWM. Note that the BP-based algorithms are simply parallel algorithms to compute the MWM: the total amount of computation, or the total number of messages needed to be exchanged, is still $O(N^3)$, but is distributed evenly across the input and the output ports (*i.e.*, $O(N^2)$ work for each input/output port). It was shown

in [2] that BP can also be used to boost the performance of other (non-BP-based) distributed iterative algorithms such as iLQF [26]. However, the “BP assistance” part alone has a total computational complexity of $O(N^2)$, or $O(N)$ per port.

Recently, a parallel crossbar scheduling algorithm based on the approach of edge coloring was proposed in [40]. However, it is a *batch scheduling* algorithm [1], in which packets are grouped into batches based on their arrival times and the matching decisions are computed on a per-batch basis. Since the duration of a batch typically spans many time slots, and a packet arriving at the beginning of a batch (*i.e.*, right after the cutoff time) has to wait till the end of the batch to be scheduled, batch scheduling algorithms typically results higher packet delays than those that do not use batching. Indeed, although this algorithm has a time complexity of $O(\log^2 N)$ per batch when using a batch size of $O(\log N)$ – or $O(\log N)$ computation per time slot (same as in SERENADE) – it cannot achieve 100% throughput, and its delay performance appears to be much worse than that of SERENA.

8.2 Wireless Transmission Scheduling

Transmission scheduling in wireless networks with primary interference constraints [30] shares a common algorithmic problem with crossbar scheduling: to compute a good matching for each “time slot”. The matching computation in the former case is however more challenging, since it needs to be performed over a general graph that is not necessarily bipartite. Several wireless transmission scheduling solutions were proposed in the literature [7, 8, 16, 20, 23, 30] that are based on distributed computation of matchings in a general graph.

Most of these solutions tackle the underlying distributed matching computation problem using an adaptation/extension of either [19] (used in [7, 16, 20]), or [18] (used in [8, 23]). In [19], a parallel randomized algorithm was proposed that outputs a maximal matching with expected runtime $O(\log |E|)$, where $|E|$ is the number of edges in the graph. This computational complexity, translated into our crossbar scheduling context, is $O(\log N)$. However, such maximal matching algorithms are known to only guarantee at least 50% throughput [28]. The work of Hoepman [18] converts an earlier sequential algorithm for computing approximate MWM [32] to a distributed algorithm. However, the distributed algorithm in [18], like its sequential version [32], can only guarantee to find a matching whose weight is at least half of that of the MWM, and hence can only guarantee at least 50% throughput also. In comparison, all SERENADE variants can empirically and/or provably guarantee 100% throughput, just like their sequential version SERENA.

The only exception, to distributed matching algorithms being based on either [19] or [18], is [30], in which the scheduling algorithm, called MIX, is arguably a distributed version of the MERGE procedure in SERENA, albeit in the wireless networking context. The objective of MIX is to compute an approximate MWM for simultaneous non-interfering wireless transmissions of packets, where the weight of a directed edge (say a wireless link from a node X to a node Y) is the length of the VOQ at X for packets destined for Y , in the SERENA manner: MERGE

the matching used in the previous time slot with a new random matching. Unlike in SERENA, however, neither matching has to be full and the connectivity topology is generally not bipartite in a wireless network, and hence the graph resulting from the union of the two matchings can contain both cycles and paths.

Like SERENADE, MIX also has three variants. As we will explain in [Appendix G](#) in details, all three variants compute the total – or equivalently the average – green and red weights of each cycle or path either by linearly traversing the cycle or path, or via a gossip algorithm [6]; they all try to mimic SERENA in a wireless network and have a time complexity at least $O(N)$, as compared to $O(\log N)$ for SERENADE. To summarize, they are clearly all “wireless SERENA”, not “wireless SERENADE”.

9 Conclusion

In this paper, we propose SERENADE, a suite of three parallel algorithm variants that can, with a time complexity of only $O(\log N)$ per port, either exactly or approximately emulate SERENA, a centralized algorithm with $O(N)$ time complexity. Through extensive simulations, we demonstrate that both C-SERENADE and O-SERENADE can achieve 100% throughput empirically. We also demonstrate that O-SERENADE has delay performances either similar to or better than those of SERENA, under various traffic load conditions, and that C-SERENADE has similar delay performances as SERENA under heavy traffic loads.

References

- [1] G. Aggarwal, R. Motwani, D. Shah, and A. Zhu. Switch scheduling via randomized edge coloring. In *Proceedings of the IEEE FOCS*, pages 502–512, Oct 2003.
- [2] S. Atalla, D. Cuda, P. Giaccone, and M. Pretti. Belief-propagation-assisted scheduling in input-queued switches. *IEEE Trans. Comput.*, 62(10):2101–2107, Oct. 2013.
- [3] H. Attiya and J. Welch. *Distributed computing: fundamentals, simulations, and advanced topics*, volume 19. John Wiley & Sons, 2004.
- [4] M. Bayati, B. Prabhakar, D. Shah, and M. Sharma. Iterative scheduling algorithms. In *Proceedings of the IEEE INFOCOM*, pages 445–453, Anchorage, AK, USA, May 2007.
- [5] M. Bayati, D. Shah, and M. Sharma. Max-product for maximum weight matching: Convergence, correctness, and lp duality. *IEEE Trans. Inf. Theory*, 54(3):1241–1251, Mar. 2008.

- [6] S. Boyd, A. Ghosh, B. Prabhakar, and D. Shah. Gossip algorithms: design, analysis and applications. In *Proceedings of the IEEE INFOCOM*, volume 3, pages 1653–1664 vol. 3, March 2005.
- [7] P. Chaporkar, K. Kar, X. Luo, and S. Sarkar. Throughput and fairness guarantees through maximal scheduling in wireless networks. *IEEE Trans. Inf. Theory*, 54(2):572–594, Feb 2008.
- [8] L. Chen, S. H. Low, M. Chiang, and J. C. Doyle. Cross-layer congestion control, routing and scheduling design in ad hoc wireless networks. In *Proceedings of the IEEE INFOCOM*, pages 1–13, April 2006.
- [9] S. Connor and G. Fort. State-dependent foster-lyapunov criteria for subgeometric convergence of markov chains. *Stochastic Processes and their Applications*, 119(12):4176 – 4193, 2009.
- [10] A. Edelman. Parallel prefix. http://courses.csail.mit.edu/18.337/2004/book/Lecture_03-Parallel_Prefix.pdf, 2004.
- [11] J. Edmonds and R. M. Karp. Theoretical improvements in algorithmic efficiency for network flow problems. *Journal of the ACM*, 19(2):248–264, Apr. 1972.
- [12] M. Fayyazi, D. Kaeli, and W. Meleis. Parallel maximum weight bipartite matching algorithms for scheduling in input-queued switches. In *Proceedings of the IEEE IPDPS*, pages 4–11, Santa Fe, NM, USA, Apr. 2004.
- [13] J. B. Fraleigh. *A First Course in Abstract Algebra*. Pearson, 7th edition, 2002. Theorem 9.8 on Page 89.
- [14] P. Giaccone, B. Prabhakar, and D. Shah. Randomized scheduling algorithms for high-aggregate bandwidth switches. *IEEE J. Sel. Areas Commun.*, 21(4):546–559, May 2003.
- [15] L. Gong, P. Tune, L. Liu, S. Yang, and J. J. Xu. Queue-proportional sampling: A better approach to crossbar scheduling for input-queued switches. In *Proceedings of the ACM SIGMETRICS*, SIGMETRICS ’17 Abstracts, pages 4–4, New York, NY, USA, 2017. ACM.
- [16] A. Gupta, X. Lin, and R. Srikant. Low-complexity distributed scheduling algorithms for wireless networks. *IEEE/ACM Trans. Netw.*, 17(6):1846–1859, Dec 2009.
- [17] G. R. Gupta, S. Sanghavi, and N. B. Shroff. Node weighted scheduling. In *Proceedings of the ACM SIGMETRICS*, pages 97–108, Seattle, WA, USA, Jun. 2009.
- [18] J.-H. Hoepman. Simple distributed weighted matchings. *eprint arXiv:cs/0410047*, Oct 2004, cs/0410047.

- [19] A. Israel and A. Itai. A fast and simple randomized parallel algorithm for maximal matching. *Inf. Process. Lett.*, 22(2):77–80, February 1986.
- [20] B. Ji, C. Joo, and N. B. Shroff. Delay-based back-pressure scheduling in multihop wireless networks. *IEEE/ACM Trans. Netw.*, 21(5):1539–1552, Oct 2013.
- [21] M. Karol, M. Hluchyj, and S. Morgan. Input versus output queueing on a space-division packet switch. *IEEE Trans. Commun.*, 35(12):1347–1356, Dec. 1987.
- [22] R. E. Ladner and M. J. Fischer. Parallel prefix computation. *J. ACM*, 27(4):831–838, Oct 1980.
- [23] X. Lin and N. B. Shroff. The impact of imperfect scheduling on cross-layer rate control in wireless networks. In *Proceedings of the IEEE INFOCOM*, volume 3, pages 1804–1814 vol. 3, March 2005.
- [24] N. A. Lynch. *Distributed Algorithms*. Morgan Kaufmann Publishers Inc., San Francisco, CA, USA, 1996.
- [25] V. A. Malyšev and M. V. Men’sikov. Ergodicity, continuity and analyticity of countable markov chains. *Trudy Moskovskogo Matematicheskogo Obshchestva*, pages 3–48, 1979.
- [26] N. McKeown. *Scheduling Algorithms for Input-Queued Cell Switches*. PhD thesis, University of California at Berkeley, May 1995.
- [27] N. McKeown. The iSLIP scheduling algorithm for input-queued switches. *IEEE/ACM Trans. Netw.*, 7(2):188–201, Apr. 1999.
- [28] N. McKeown, A. Mekkittikul, V. Anantharam, and J. Walrand. Achieving 100% throughput in an input-queued switch. *IEEE Trans. Commun.*, 47(8):1260–1267, Aug. 1999.
- [29] A. Mekkittikul and N. McKeown. A practical scheduling algorithm to achieve 100% throughput in input-queued switches. In *Proceedings of the IEEE INFOCOM*, pages 792–799 vol.2, Mar. 1998.
- [30] E. Modiano, D. Shah, and G. Zussman. Maximizing throughput in wireless networks via gossiping. In *Proceedings of the ACM SIGMETRICS joint international conference on Measurement and modeling of computer systems*, SIGMETRICS ’06/Performance ’06, pages 27–38, New York, NY, USA, 2006. ACM.
- [31] R. Perlman. *Interconnections (2Nd Ed.): Bridges, Routers, Switches, and Internetworking Protocols*. Addison-Wesley Longman Publishing Co., Inc., Boston, MA, USA, 2000.

- [32] R. Preis. Linear time $1/2$ -approximation algorithm for maximum weighted matching in general graphs. In *Proceedings of the 16th Annual Conference on Theoretical Aspects of Computer Science*, STACS'99, pages 259–269, Berlin, Heidelberg, 1999. Springer-Verlag.
- [33] D. Shah, P. Giaccone, and B. Prabhakar. Efficient randomized algorithms for input-queued switch scheduling. *IEEE Micro*, 22(1):10–18, Jan. 2002.
- [34] D. Shah and D. Wischik. Optimal scheduling algorithms for input-queued switches. In *Proceedings of the IEEE INFOCOM*, pages 1–11, Barcelona, Spain, Apr. 2006.
- [35] J. Shin and T. Suk. Scheduling using Interactive Optimization Oracles for Constrained Queueing Networks. *ArXiv e-prints*, Jul 2014, 1407.3694.
- [36] J. Shin and T. Suk. Scheduling using interactive oracles: Connection between iterative optimization and low-complexity scheduling. In *Proceedings of the ACM SIGMETRICS*, SIGMETRICS '14, pages 577–578, New York, NY, USA, 2014. ACM.
- [37] T. Tao. Cycles of a random permutation, and irreducible factors of a random polynomial. <https://goo.gl/qpDPJo>, July 2015. Accessed on December 14, 2016.
- [38] L. Tassiulas. Linear complexity algorithms for maximum throughput in radio networks and input queued switches. In *Proceedings of the IEEE INFOCOM*, pages 533–539, San Francisco, CA, USA, Mar. 1998.
- [39] L. Tassiulas and A. Ephremides. Stability properties of constrained queueing systems and scheduling policies for maximum throughput in multihop radio networks. *IEEE Trans. Autom. Control*, 37(12):1936–1948, Dec. 1992.
- [40] L. Wang, T. Ye, T. T. Lee, and W. Hu. Parallel scheduling algorithm based on complex coloring for input-queued switches. *CoRR*, abs/1606.07226, 2016.
- [41] S. Ye, T. Shen, and S. Panwar. An $O(1)$ scheduling algorithm for variable-size packet switching systems. In *Proceedings of the 48th Annual Allerton Conference*, pages 1683–1690, Sept. 2010.

A Parallelized Population

As explained in §3.1, the new random matching $A'(t)$ derived from the *arrival graph*, which is in general a partial matching, has to be populated into a full matching $R(t)$ before it can be merged with $S(t-1)$, the matching used in the previous time slot. SERENADE parallelizes this POPULATE procedure, *i.e.*, the round-robin pairing of unmatched input ports in $R(t)$ with unmatched output ports in $R(t)$, so that the computational complexity for each input port is $O(\log N)$, as follows.

Suppose that each unmatched port (input port or output port) knows its own ranking, *i.e.*, the number of unmatched ports up to itself (including itself) from the first one (we will show later how each unmatched port can obtain its own ranking). Then, each unmatched input port needs to obtain the identity of the unmatched output port with the same ranking. This can be done via 3 message exchanges as follows. Each pair of unmatched input and output ports “exchange” their identities through a “broker”. More precisely, the j^{th} unmatched input port (*i.e.*, unmatched input port with ranking j) first sends its identity to input port j (*i.e.*, the broker). Then, the j^{th} unmatched output port also sends its identity to input port j (*i.e.*, the broker). Finally, input port j (*i.e.*, the broker) sends the identity of the output port with ranking j to the input port (with ranking j). Thus, the input port learns the identity of the corresponding output port. Note that, since every pair of unmatched input port and output port has its unique ranking, thus they would have different “brokers”. Therefore, all pairs can simultaneously exchange their messages without causing any congestion (*i.e.*, a port sending or receiving too many messages).

It remains to parallelize the computation of ranking each port (input port or output port). This problem can be reduced to the parallel prefix sum problem [10] as follows. Here, we will only show how to compute the rankings of input ports in parallel; that for output ports is identical. Let $B[1..N]$ be a bitmap that indicates whether input port i is unmatched (when $B[i] = 1$) or not (when $B[i] = 0$). Note that, this bitmap is distributed, that is, each input port i only has a single bit $B[i]$. For $i = 1, 2, \dots, N$, denote as r_i the ranking of input port i . It is clear that $r_i = \sum_{k=1}^i B[k]$, for any $1 \leq i \leq N$. In other words, the N terms r_1, r_2, \dots, r_N are the prefix sums of the N terms $B[1], B[2], \dots, B[N]$. Using the Ladner-Fischer parallel prefix-sum algorithm [22], we can obtain these N prefix sums r_1, r_2, \dots, r_N in $O(\log N)$ time (per port) using $2N$ processors (one at each input or output port).

B Making Do with Less

As explained in §4.1, after $1 + \log_2 N$ iterations of SERENADE-common, each vertex i knows only the following information:

- $\sigma^{2^k}(i)$, $w_r(i \rightsquigarrow \sigma^{2^k}(i))$, and $w_g(i \rightsquigarrow \sigma^{2^k}(i))$, or equivalently $\phi_{k+}^{(i)}$, for $k = 0, 1, 2, \dots, \log_2 N$;
- $\sigma^{-2^k}(i)$, $w_r(\sigma^{-2^k}(i) \rightsquigarrow i)$, and $w_g(\sigma^{-2^k}(i) \rightsquigarrow i)$, or equivalently $\phi_{k-}^{(i)}$, for $k = 0, 1, 2, \dots, \log_2 N$.

Clearly, the total amount of this information is $O(\log N)$. In both C-SERENADE and O-SERENADE, each vertex i learns no additional information afterwards. In E-SERENADE, the vertices along the path of the binary search may each learn $O(1)$ additional information (see §5.3.1). Therefore, in all three SERENADE variants, the total amount of information each vertex i knows is $O(\log N)$.

In comparison, in SERENA, each vertex i knows much more information. More specifically, each vertex i knows the following information: $\sigma^m(i)$, $w_r(i \rightsquigarrow \sigma^m(i))$, and $w_g(i \rightsquigarrow \sigma^m(i))$ for $m = 0, 1, 2, \dots, N$. The total amount of this information is $O(N)$.

Despite this significant information disadvantage, E-SERENADE emulates SERENA exactly, and as shown in §7.2, O-SERENADE empirically has similar delay performance as SERENA under various workload conditions.

C Explanation of The Tree Ideal Situations

In the first situation (with equation $i = \sigma^{2^n}(i)$), we know that l (*i.e.*, the length of the cycle to which vertex i belongs) divides 2^n because l is the smallest positive integer for such an equation to hold. This implies that $l = 2^{n'}$ for some nonnegative n' . Hence the vertex i knows both $w_g(i \rightsquigarrow \sigma^l(i))$ and $w_r(i \rightsquigarrow \sigma^l(i))$ because both belong to the knowledge set $\phi_{n'+}^{(i)}$.

In the second situation (with equation $\sigma^{2^n}(i) = \sigma^{2^m}(i)$), we have $i = \sigma^{(2^m - 2^n)}(i)$ (by applying the operator σ^{-2^n} to both sides of the equation), so l divides $2^m - 2^n$ for the same reason as in the first situation. Suppose $\kappa l = 2^m - 2^n$, where κ is a positive integer. We know the $(2^m - 2^n)$ -edge-long walk $\sigma^{2^n}(i) \rightsquigarrow \sigma^{2^m}(i)$ “coils around” the cycle (of length l) precisely κ times, and so its green weight $w_g(\sigma^{2^n}(i) \rightsquigarrow \sigma^{2^m}(i))$ (or red weight $w_r(\sigma^{2^n}(i) \rightsquigarrow \sigma^{2^m}(i))$) is κ times that of the cycle. Since vertex i can obtain $w_g(\sigma^{2^n}(i) \rightsquigarrow \sigma^{2^m}(i))$ (and similarly obtain $w_r(\sigma^{2^n}(i) \rightsquigarrow \sigma^{2^m}(i))$) via subtracting $w_g(i \rightsquigarrow \sigma^{2^m}(i))$ ($\in \phi_{m+}^{(i)}$) by $w_g(i \rightsquigarrow \sigma^{2^n}(i))$ ($\in \phi_{n+}^{(i)}$), it knows whether $w_g(i \rightsquigarrow \sigma^l(i))$ or $w_r(i \rightsquigarrow \sigma^l(i))$ is larger. In the third situation (with equation $\sigma^{-2^n}(i) = \sigma^{2^m}(i)$), we similarly have $i = \sigma^{(2^m + 2^n)}(i)$, so l divides $2^m + 2^n$. The rest of reasoning is the same as before.

D Ouroboros Statistics

In this section, we analyze, given a switch size N , the probability for an (arbitrary) input port i to be on an ouroboros cycle of σ (an ideal situation), and that for σ to be ouroboros (the best-case scenario). It however makes no sense, if possible at all, to calculate these two probability values because both are functions of (the real-world) σ , which is itself a “nasty” random variable that depends on both the packet arrival and the matching decision histories up to the current time slot t . Hence, we calculate both for a different and simpler σ that is “sampled” uniformly at random from the set of $N!$ permutation functions over the range $\{1, 2, \dots, N\}$. Note that we are not at an advantage to instead use such a uniform random σ because it is arguably the worst-case scenario in the sense these two probability values are generally larger (better) for a real-world σ , as we will explain shortly. On the other hand, we are not at a disadvantage either, because it can be shown that, under uniform traffic (matrix), σ_r is precisely a uniform random permutation, and hence so is $\sigma = \sigma_g^{-1} \circ \sigma_r$.

When σ is a uniform random permutation, the aforementioned first probability (for any vertex i to be on an ouroboros cycle) is simply $\frac{\mathcal{O}_N}{N}$, the number of ouroboros numbers (*w.r.t.* N) divided by N , due to the following fact.

Fact 3 ([37]) *Let $\pi : \{1, \dots, N\} \rightarrow \{1, \dots, N\}$ be a uniform random permutation over $\{1, \dots, N\}$. Then, in the cycle decomposition of π , for any arbitrary $i \in \{1, \dots, N\}$, the probability that i lies on a cycle of length l is $\frac{1}{N}$, for $l = 1, 2, \dots, N$.*

Since \mathcal{O}_N scales roughly as $O(\log^2 N)$, as explained in §4.2, this probability \mathcal{O}_N/N becomes smaller, albeit sub-linearly, when N grows larger. As to the aforementioned second probability (for σ to be ouroboros), even for a uniform random σ , it does not have a closed form, but can be computed through Monte-Carlo simulations. The third row of Table 1 shows the second probability values when N varies from 64 to 1024. It clearly shows that the second probability drops super-linearly *w.r.t.* N (*i.e.*, at a faster rate than N increases).

However, the drop of both probabilities when N becomes larger does not “doom” the delay performances of C-SERENADE and O-SERENADE algorithms when N is large, due to the following two facts that we have shown, through both intuitive reasoning and simulations (up to $N = 128$ due to the prohibitively high amount of computation needed to simulate larger N values). First, under O-SERENADE, vertices on a *non-ouroboros* cycle will, with high probability, also choose the heavier sub-matching, especially when the green and the red weights of the sub-matchings are far apart. Second, under C-SERENADE, during each time slot t , the weight (*i.e.*, quality) of the matching $S(t)$ guarantees not to drop much (if at all) compared to that of $S(t-1)$, and can increase, if there is one or more ouroboros cycles in the corresponding (to t) permutation.

To explain why the uniform random permutation is arguably the worst-case scenario, we need the following fact about ouroboros numbers (*w.r.t.* N): They concentrate most heavily near 1, and to a lesser degree near N . For example, when $N = 64$, all numbers 1 through 18 are ouroboros numbers; so are 64, 63, 62, and 60. Now we claim that the length of a cycle uniformly randomly sampled (by vertex i) from a real-world $\sigma (= \sigma_g^{-1} \circ \sigma_r)$ usually tends to stochastically smaller than the uniform distribution on $\{1, 2, \dots, N\}$. This claim, combined with the fact that all short cycles are ouroboros (due to the aforementioned high concentration of ouroboros numbers near 1), explains why the real-world σ usually has more vertices lying on ouroboros cycles than a uniform random permutation. This claim itself is true because the permutation σ_g (corresponding to the matching S_g) used in the previous time slot and the permutation σ_r (corresponding to the matching S_r) derived from the arrival graph are usually positively correlated. For example, a long VOQ (say corresponding to a “heavy” edge e at the input port I_e) that was served in the previous time slot (*i.e.*, $e \in S_g$), is more likely (than a random VOQ) to have a packet arrival in the current time slot ($e \in S_r$), because a very likely reason for this VOQ to become long is its high packet arrival rate; in this case, in the cycle decomposition graph of σ , the vertex I_e lies on a cycle of length 1 (*i.e.*, by itself).

E Check for Ouroboros

As stated in the last paragraph of §4.3.3, at the end of every iteration k , the vertex i checks whether itself is on an ouroboros cycle, in view of the new knowledge sets $\phi_{k+}^{(i)}$ and $\phi_{k-}^{(i)}$. If it is, then the SERENADE-common algorithm halts on vertex i and all other vertices on the same cycle as vertex i , and a sub-matching decision is made within this cycle. As explained earlier, to check that, the vertex i needs to check whether $\sigma^{2^k}(i)$ (a part of knowledge set $\phi_{k+}^{(i)}$) or $\sigma^{-2^k}(i)$ (a part of knowledge set $\phi_{k-}^{(i)}$) matches with any of the identities in any knowledge sets that learned before iteration k , *i.e.*, $\{\phi_{j+}^{(i)}\}_{j=0}^{k-1}$ and $\{\phi_{j-}^{(i)}\}_{j=0}^{k-1}$. For succinctness of presentation, we only explain how to check for $\sigma^{2^k}(i)$, since how to check for $\sigma^{-2^k}(i)$ is similar, and we only explain how to check against $\{\phi_{j+}^{(i)}\}_{j=0}^{k-1}$, since how to check against $\{\phi_{j-}^{(i)}\}_{j=0}^{k-1}$ is similar. A naive way to carry out this search task would be to “linearly” scan through the identities $\{\sigma^{2^j}(i)\}_{j=0}^{k-1}$ (contained respectively in the existing knowledge sets $\{\phi_{j+}^{(i)}\}_{j=0}^{k-1}$). However, its computational complexity would be $O(\log N)$ per iteration, or $O(\log^2 N)$ in total.

We can reduce this complexity to $O(1)$ (per port) per iteration, or $O(\log N)$ in total, using a simple data structure, as follows. As explained earlier, we only describe how to search $\sigma^{2^k}(i)$ against $\{\phi_{j+}^{(i)}\}_{j=0}^{k-1}$. The data structure consists of two arrays $D[0..\log_2 N]$ and $B[1..N]$. Each array entry $D[k]$ stores $\sigma^{2^k}(i)$, along with the rest of $\phi_{k+}^{(i)}$, so our search task is to look for the identity $\sigma^{2^k}(i)$ in this array. This search task can be carried out in $O(1)$ time with help from array B . Each array entry $B[i']$ stores the “inverted index” of the identity i' in array D as follows: If $i' = \sigma^{2^{k'}}(i)$ then $B[i'] = k' + 1$; otherwise, $B[i'] = 0$. Hence B is a very “sparse” array in which at most $1 + \log_2 N$ entries (out of a total of N entries) are nonzero. To check whether $\sigma^{2^k}(i)$ matches with any of the identities in D , we need only to check whether $B[\sigma^{2^k}(i)]$ is 0, which is clearly an $O(1)$ operation.

Note that we need to reset the values of all N entries of B to 0 at the end of a matching computation. The computational complexity of the reset is $O(\log N)$ (instead of $O(N)$) because each nonzero entry of B is pointed to by an entry in array D , which has a total of $1 + \log_2 N$ entries. Hence the total computational complexity for each vertex i to check whether it is on an ouroboros cycle is $O(\log N)$.

F An Idempotent Trick

As mentioned in §5.2.1, there is an alternative solution to the consistency problem that does not require leader election, using a standard “idempotent trick” that was used in [30] to solve a similar problem. To motivate this trick, we zoom in on the example shown in Figure 5. Both the consistency problem and the absolute correctness problem above can be attributed to the fact that the (green or red) weights of some edges are accounted for (*i.e.*, added to the total) κ

times, while those of others $\kappa - 1$ times. For example, in $3 \rightsquigarrow \sigma^8(3)$, the (green or red) weights of edges (3, 4) and (4, 7) are accounted for 3 times, while that of edge (7, 3) 2 times. Since the “+” operator is not idempotent (so adding a number to a counter κ times is not the same as adding it $\kappa - 1$ times), the total (green or red) weight of the walk obtained this way does not perfectly track that of the cycle.

The “idempotent trick” is to use, instead of the “+” operator, a different and idempotent operator MIN to arrive at an estimation of the total green (or red) weight; the MIN is idempotent in the sense the minimum of a multi-set (of real numbers) M is the same as that of the set of distinct values in M . The idempotent trick works, in this O-SERENADE context, for a set of edges e_1, e_2, \dots, e_Z that comprise a non-ouroboros cycle with green weights w_1, w_2, \dots, w_Z respectively, as follows; the trick works in the same way for the red weights. Each edge e_ζ “modulates” its green weight w_ζ onto an exponential random variable X_ζ with distribution $F(x) = 1 - e^{-x/w_\zeta}$ (for $x > 0$) so that $E[X_\zeta] = w_\zeta$. Then the green weight of every walk W on this non-ouroboros cycle can be encoded as $MIN\{X_\zeta | e_\zeta \in W\}$. It is not hard to show that we can compute this MIN encoding of every 2^d -edge-long walk $i \rightsquigarrow \sigma^{2^d}(i)$ by SERENADE-common in the same inductive way we compute the “+” encoding. For example, under the MIN encoding, [line 1](#) in [Procedure 1](#) becomes “Send to i_U the value $MIN\{X_\zeta | e_\zeta \in i \rightsquigarrow \sigma^{2^{k-1}}(i)\}$ ”. However, unlike the “+” encoding, which requires the inclusion of only 1 “codeword” in each message, the MIN encoding requires the inclusion of $O(N \log N)$ i.i.d. “codewords” in each message in order to ensure sufficient estimation accuracy [\[30\]](#).

G SERENADE vs. MIX

In this section, we describe the three variants of MIX [\[30\]](#) in detail. The first variant, which is centralized and idealized, computes the total green and red weights of each cycle or path by “linearly” traversing the cycle or path. Hence it has a time complexity of $O(N)$, where N is the number of nodes in a wireless network. This idealized variant is however impractical because it requires the complete knowledge of the connectivity topology of the wireless network.

The second variant removes this infeasible requirement and hence is practical. It estimates and compares the *average* green and red weights of each cycle or path (equivalent to comparing the total green and red weights) using a synchronous iterative gossip algorithm proposed in [\[6\]](#). In this gossip algorithm, each node (say X) is assigned a green (or red) weight that is equal to the weight of the edge that uses X as an endpoint and belongs to the matching used in the previous time slot (or in the new random matching); in each iteration, each node attempts to pair with a random neighbor and, if this attempt is successful, both nodes will be assigned the same red (or green) weight equal to the average of their current red (or green) weights. The time complexity of each MERGE is $O(l^2 N \log N)$, since this gossip algorithm requires $O(l^2 N \log N)$ iterations [\[30\]](#) for the average red (or green) weight estimate to be close to the actual average with high probability. Here l is the length of the longest path or cycle.

The third (practical) variant, also a gossip-based algorithm, employs the aforementioned “idempotent trick” (see [Appendix F](#)) to estimate and compare the *total* green and red weights of each cycle or path. This idempotent trick reduces the convergence time (towards the actual total weights) to $O(l)$ iterations, but as mentioned earlier requires each pair of neighbors to exchange a large number ($O(N \log N)$ to be exact) of exponential random variables during each message exchange. Since l is usually $O(N)$ in a random graph, the time complexity of this algorithm can be considered $O(N)$.

H Stability Proof of Hybrid SERENADE Schemes

In this section, we “prove” that the hybrid SERENADE schemes (*i.e.*, SC-SERENADE, and SO-SERENADE) are stable under any *i.i.d.* arrival processes that are admissible. In [Appendix H.1](#), we introduce some background and notations that we need in our stability “proofs”. In [Appendix H.2](#), we describe a theorem (*i.e.*, [Theorem 1](#)) proven in [38], which will be used (or slightly extended) for “proving” the stability of SC-SERENADE and SO-SERENADE. Then, we state the stability “proof” for the hybrid schemes. Finally, we explain the difficulty for proving the stabilities of C-SERENADE and O-SERENADE.

H.1 Background and Notations

Each matching can be represented as an $N \times N$ sub-permutation matrix $S = (s_{ij})$, in which $s_{ij} = 1$ if and only if the input port i is matched with the output port j . Let $Q(t) = (q_{ij}(t))$ be the $N \times N$ queue length matrix where $q_{ij}(t)$ is the length of the j^{th} VOQ at input port i during time slot t . We “flatten” it into an N^2 -dimensional vector (say in the row-major order), and flatten the above-defined schedule (matching) matrix S in the same manner. Then the weight of the matching S , with respect to $Q(t)$, is equal to their inner product $\langle Q(t), S \rangle$.

Like in [39], we assume that packet arrivals to any VOQ follow a discrete *i.i.d.* arrival process with finite second moment, and the arrival processes to different VOQs are mutually independent. Let λ_{ij} be the average packet arrival rate to the j^{th} VOQ at input port i , for $1 \leq i, j \leq N$. These N^2 packet arrival rates naturally form the traffic matrix $(\lambda_{ij})_{1 \leq i, j \leq N}$. This traffic matrix is called *admissible*, if $\sum_{j=1}^N \lambda_{ij} < 1$, for any $1 \leq i \leq N$ and $\sum_{i=1}^N \lambda_{ij} < 1$, for any $1 \leq j \leq N$.

H.2 Stability of Hybrid SERENADE Schemes

H.2.1 An Important Theorem

The following theorem, proven in [38], concerns the stability of a family of crossbar scheduling algorithms which are non-degenerative (see [Definition 1](#)) and satisfy the *Property P* (see [Definition 2](#)).

Theorem 1 (Proposition 1 in [38]) *Given any non-degenerative (defined below) randomized crossbar scheduling algorithm satisfying Property P (defined below), the joint stochastic process $\{(Q(t), S(t))\}_{t=0}^{\infty}$ is an ergodic Markov chain under any admissible i.i.d. arrival process $A(t)$, and thereafter, the queueing process $\{Q(t)\}_{t=0}^{\infty}$ converges in distribution to a random vector \hat{Q} with finite expectation, i.e.,*

$$\mathbb{E}[\|\hat{Q}\|_1] < \infty,$$

where $\|\cdot\|_1$ is the 1-norm.

Definition 1 (Non-degenerative) *A randomized crossbar scheduling algorithm is non-degenerative if given any time slot $t \geq 1$, it guarantees*

$$\langle Q(t), S(t) \rangle \geq \langle Q(t), S(t-1) \rangle. \quad (1)$$

Definition 2 (Property P [38]) *A randomized crossbar scheduling algorithm satisfies Property P, if at any time slot t , there exists a constant $\delta > 0$ independent of t and the queue length vector $Q(t)$ such that,*

$$\mathcal{P}[\langle Q(t), S(t) \rangle = W_{Q(t)}] \geq \delta, \quad (2)$$

where $W_{Q(t)}$ is the weight of the maximum weight matching at time slot t .

Note that, [Theorem 1](#) is applicable to E-SERENADE (or SERENA) for two reasons. First, MERGE procedure guarantees that it is *non-degenerative*, since the merged matching S (i.e., $S(t)$) is at least as heavy as both S_g (i.e., $S(t-1)$, the matching used in the previous time slot) and S_r (i.e., $R(t)$, the full matching derived and populated from the arrival graph $A(t)$). Second, it satisfies *Property P*, since the arrival graph $A(t)$ (and hence $R(t)$) has a constant probability (i.e., independent of t and $Q(t)$) of being a Maximum Weighted Matching, and the MERGE procedure ensures that the merged matching remains an MWM whenever $R(t)$ is.

H.2.2 Stability of SC-SERENADE and SO-SERENADE

Now we explain why [Theorem 1](#) is also applicable to SC-SERENADE. Without loss of generality, we assume this SC-SERENADE mixes 1% of E-SERENADE with 99% of C-SERENADE. We note that C-SERENADE is non-degenerative, because the switch conservatively uses sub-matchings of the old matching $S(t-1)$ – and hence has the same weight w.r.t. $Q(t)$ – unless it is sure those of the new matching $R(t)$ are heavier. Hence, SC-SERENADE is non-degenerative (since E-SERENADE is non-degenerative, as we have just shown). Now it remains only to show that SC-SERENADE satisfies Property P. The argument is straightforward: Since SC-SERENADE runs E-SERENADE with probability 0.01 (i.e., 1% of time as assumed earlier), which as just explained has at least a constant probability (say δ') of outputting an MWM, SC-SERENADE has at least a constant probability (precisely $0.01\delta'$) of outputting an MWM (i.e., satisfies *Property P*).

It is slightly trickier to prove the stability of SO-SERENADE (whose O-SERENADE is with the COW modification), since O-SERENADE, even with the COW modification, is not

non-degenerative. However, it is straightforward to extend [Theorem 1](#) to scheduling algorithms that are *C-degenerative* (see [Definition 3](#) below) and satisfy the *Property P*, by modifying its proof slightly. Indeed, similar modifications (for accommodating such a constant C) are used in the proofs of [Theorem 4](#) in [\[29\]](#) and [Lemma 1](#) in [\[14\]](#).

Definition 3 (*C*-degenerative) *A randomized crossbar scheduling algorithm is called *C*-degenerative (i.e., by at most a constant value), if there exists a constant $C > 0$ such that for any time slot $t \geq 1$, it guarantees*

$$\langle Q(t), S(t) \rangle \geq \langle Q(t), S(t-1) \rangle - C. \quad (3)$$

The O-SERENADE part (with COW modification) of SO-SERENADE is *C-degenerative*, because the weight of the matching $S(t)$ – with respect to $Q(t)$ – is at most NW smaller than that of $S(t-1)$, where W is the COW threshold defined in [§6](#). Hence, SO-SERENADE is *C-degenerative*. Since SO-SERENADE also satisfies *Property P* for the same reason SC-SERENADE does, SO-SERENADE is stable under any admissible *i.i.d.* traffic arrival.

H.2.3 Difficulties in Proving the Stability of C-SERENADE and O-SERENADE

It appears difficult to prove the stability of C-SERENADE for the following reasons. First, it is not clear whether *Property P* still holds under C-SERENADE, and if it does, how to prove it. In SERENA, since the new random matching $R(t)$ is uniformly random, it has a constant probability to be an MWM so that, after the MERGE, it remains an MWM. However, this is no longer true in C-SERENADE, because the union graph resulting from the MERGE may contain a non-ouroboros cycle that prevents the heavier sub-matching that belongs to the new random matching from being chosen, as C-SERENADE conservatively sticks to the old sub-matching in such a case.

Furthermore, because of this conservative behavior, in this case C-SERENADE could get stuck at (i.e., keep outputting) a local MWM, the weight of which is smaller than that of a (global) MWM by at least a constant fraction, for a “very long time.” In particular, this “very long time” can be proportional to the weight of the global MWM at the time C-SERENADE became stuck at a local MWM, and hence can exceed the length of any “single step” (say 1 trillion time slots) used in standard single-step Lyapunov stability analyses. Since the (same) stability proof ([Proposition 1](#) in [\[38\]](#)) that is used by SERENA [\[14\]](#) is based on single-step Lyapunov stability analysis, there is no way for it to work for C-SERENADE with only a minor tweak.

As readers might suspect, we had tried multi-step (and/or state-dependent) Lyapunov stability analysis [\[9, 25\]](#), but to no avail. One key difficulty we encountered was that we were not able to *rigorously* calculate or bound the probability values of various “ouroboros-related events” that lie at the heart of such analyses, due to the fact that these probability values depend on the exact value of the current (say at time slot t) matching, which in turn depends, due

to the adaptive nature of SERENA/SERENADE, on the entire history of how the VOQ length vector, a Markov chain, evolves from time 0 to t . All said, we still believe the correctness of the conjecture (that C-SERENADE can achieve 100% throughput) and that it can eventually be proven. We also believe, this proof, if found, would be contrived and long, and likely could become the subject of a separate paper.

It appears difficult to prove the stability of O-SERENADE (without COW modification) for a very different reason. Whereas it is straightforward to prove that a variant of O-SERENADE with rotating leadership⁶ possesses Property P, O-SERENADE is not C-degenerative. In particular, in O-SERENADE the weight of the entire matching could drop by a constant fraction due to a wrong decision made (by O-SERENADE) on a non-ouroboros cycle, leading to a large (*i.e.*, proportional to the current weight of MWM) positive drift (of any chosen Lyapunov function). While it is conceivably possible to bring this drift to the negative territory through a multi-step Lyapunov stability analysis [9, 25], we would have to confront the same difficulty as we encountered in multi-step Lyapunov stability analysis of C-SERENADE, namely, the probabilistic analysis of various ouroboros-related events.

Finally, we note that O-SERENADE with COW modification is C-degenerative, but does not generally possess *Property P* (just like C-SERENADE). So we are facing the same difficulty in proving its stability as in proving C-SERENADE's.

I More Evaluations

In this section, we evaluate the mean delay performances of SERENADE algorithm suite under bursty traffic (see [Appendix I.1](#)), and investigate how their mean delay performances scale with respect to N under (non-bursty) Bernoulli i.i.d. traffic (see [Appendix I.2](#)). Again, in both simulation studies (under bursty traffic and with N varying), the mean delays of C-SERENADE and SC-SERENADE are almost identical; the same can be said about O-SERENADE and SO-SERENADE. Hence we show the mean delays of only the stabilized variants (*i.e.*, SC-SERENADE and SO-SERENADE) in the following figures.

I.1 Bursty Arrivals

In real networks, packet arrivals are likely to be bursty. In this section, we evaluate the performances of SC-SERENADE, SO-SERENADE, and SERENA under heavy bursty traffic, generated by a two-state ON-OFF arrival process described in [14]. The durations of each ON (burst) stage and OFF (no burst) stage are geometrically distributed: the probabilities that the ON and OFF states last for $t \geq 0$ time slots are given by

$$P_{ON}(t) = p(1 - p)^t \text{ and } P_{OFF}(t) = q(1 - q)^t,$$

⁶During each time slot t , every vertex i is assigned a “nominee ID” $(i + t) \bmod N$, and this nominee ID, instead of the original ID i , is used for leader election.

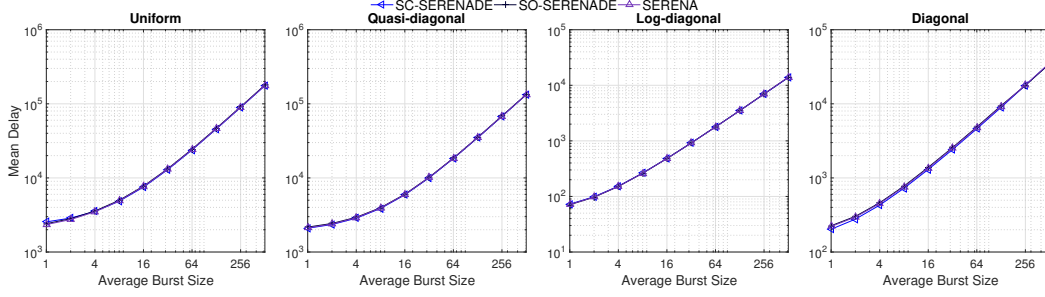


Figure 8: Mean delays of SC-SERENADE, SO-SERENADE and SERENA under the bursty arrivals with the 4 traffic load matrices.

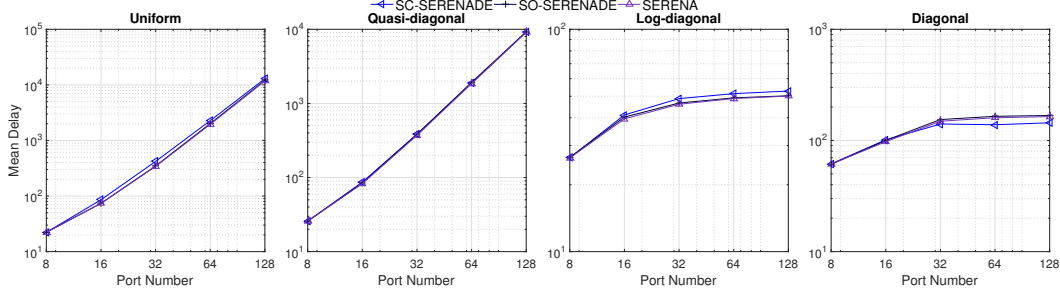


Figure 9: Mean delays v.s. port numbers under i.i.d. Bernoulli traffic arrivals with the 4 traffic load matrices.

with the parameters $p, q \in (0, 1)$ respectively. As such, the average duration of the ON and OFF states are $(1 - p)/p$ and $(1 - q)/q$ time slots respectively.

In an OFF state, an incoming packet's destination (*i.e.*, output port) is generated according to the corresponding load matrix. In an ON state, all incoming packet arrivals to an input port would be destined to the same output port, thus simulating a burst of packet arrivals. By controlling p , we can control the desired average burst size while by adjusting q , we can control the load of the traffic.

We have evaluated the mean delay performances of SC-SERENADE, SO-SERENADE, and SERENA, with the average burst size ranging from 1 to 512 packets, under heavy offered loads up to 0.95. The simulation results under the offered load of 0.95, plotted in Figure 8, show that SC-SERENADE and SO-SERENADE have almost the same mean delays as SERENA under the 4 traffic load matrices with all the burst sizes. The same observation can be made about the mean delay performances of the three algorithms under other heavy offered loads. To summarize, our simulation studies show conclusively that C-SERENADE and O-SERENADE, as well as their stabilized variants SC-SERENADE and SO-SERENADE, are able to handle bursty traffic as well as SERENA.

I.2 Delay versus Port Number

In this section, we investigate how the mean delays of the SERENADE algorithms scale with the number of input/output ports N under (non-bursty) Bernoulli i.i.d. traffic. We have simulated five different N values: $N = 8, 16, 32, 64, 128$. [Figure 9](#) compares the mean delays for SC-SERENADE and SO-SERENADE against that for SERENA, under the 4 different traffic load matrices with an offered load of 0.95. It shows that the scaling behaviors of SC-SERENADE and SO-SERENADE are almost the same as that of SERENA in terms of mean delays, for all values of N .